Journal of Visualized Experiments

Neutron Spin Echo Spectroscopy as a Unique Probe for Lipid Membrane Dynamics and Membrane-Protein Interactions

--Manuscript Draft--

Article Type:	Invited Methods Collection - JoVE Produced Video
Manuscript Number:	JoVE62396R2
Full Title:	Neutron Spin Echo Spectroscopy as a Unique Probe for Lipid Membrane Dynamics and Membrane-Protein Interactions
Corresponding Author:	Rana Ashkar Virginia Tech: Virginia Polytechnic Institute and State University Blacksburg, VA UNITED STATES
Corresponding Author's Institution:	Virginia Tech: Virginia Polytechnic Institute and State University
Corresponding Author E-Mail:	ashkar@vt.edu
Order of Authors:	Rana Ashkar
	Teshani Kumarage
	Julie Nguyen
Additional Information:	
Question	**Response**
Please indicate whether this article will be Standard Access or Open Access.	Standard Access (US$2,400)
Please specify the section of the submitted manuscript.	Biology
Please indicate the **city, state/province, and country** where this article will be **filmed**. Please do not use abbreviations.	Blacksburg, VA
Please confirm that you have read and agree to the terms and conditions of the author license agreement that applies below:	I agree to the Author License Agreement
Please provide any comments to the journal here.	
Please indicate whether this article will be Standard Access or Open Access.	Standard Access ($1400)

TITLE:

Neutron Spin Echo Spectroscopy as a Unique Probe for Lipid Membrane Dynamics and Membrane-Protein Interactions

AUTHORS AND AFFILIATIONS:

Teshani Kumarage[1,2], Julie Nguyen[1], Rana Ashkar[1,2]

[1]Department of Physics, Virginia Tech, Blacksburg, VA, USA
[2]Center for Soft Matter and Biological Physics, Virginia Tech, Blacksburg, VA, USA

Email addresses of co-authors:
Teshani Kumarage (teshani92@vt.edu)
Julie Nguyen (julie99@vt.edu)
Rana Ashkar (ashkar@vt.edu)

Corresponding author:
Rana Ashkar (ashkar@vt.edu)

KEYWORDS:

collective lipid dynamics, bending modulus, area compressibility, thickness fluctuations, membrane viscosity, selective deuteration, liposome preparation

SUMMARY:

This paper describes the protocols for sample preparation, data reduction, and data analysis in neutron spin echo (NSE) studies of lipid membranes. Judicious deuterium labeling of lipids enables access to different membrane dynamics on mesoscopic length and time scales, over which vital biological processes occur.

ABSTRACT:

Lipid bilayers form the main matrix of cell membranes and are the primary platform for nutrient exchange, protein-cell interactions, and viral budding, among other vital cellular processes. For efficient biological activity, cell membranes should be rigid enough to maintain the integrity of the cell and its compartments yet fluid enough to allow membrane components, such as proteins and functional domains, to diffuse and interact. This delicate balance of elastic and fluid membrane properties, and their impact on biological function, necessitate a better understanding of collective membrane dynamics over mesoscopic length and time scales of key biological processes, e.g., membrane deformations and protein binding events. Among the techniques that can effectively probe this dynamic range is neutron spin echo (NSE) spectroscopy. Combined with deuterium labeling, NSE can be used to directly access bending and thickness fluctuations as well as mesoscopic dynamics of select membrane features. This paper provides a brief description of the NSE technique and outlines the procedures for performing NSE experiments on liposomal membranes, including details of sample preparation and deuteration schemes, along with instructions for data collection and reduction. The paper also introduces data analysis methods used to extract key membrane parameters, such as the bending rigidity

modulus, area compressibility modulus, and in-plane viscosity. To illustrate the biological importance of NSE studies, select examples of membrane phenomena probed by NSE are discussed, namely, the effect of additives on membrane bending rigidity, the impact of domain formation on membrane fluctuations, and the dynamic signature of membrane-protein interactions.

INTRODUCTION:

The understanding of cell membranes and their function has remarkably evolved over the last few decades. The former view of cell membranes as passive lipid bilayers that define cell boundaries and house membrane proteins[1] has gradually transformed into a dynamic model in which lipid bilayers play an important role in regulating vital biological processes, including cellular signaling, molecular exchange, and protein function – to name a few[2–6]. This realization that cell membranes are highly dynamic, constantly undergoing remodeling and molecular redistribution, has urged scientific explorations beyond equilibrium structures of membranes[7–9]. Accordingly, multiple approaches have been developed to study the various dynamic modes in biological and bioinspired lipid membranes. To date, the majority of these studies have primarily focused on diffusive molecular motions[10–13] and macroscopic shape fluctuations[14–16], leaving a significant gap in understanding intermediate membrane dynamics, i.e., collective fluctuations of lipid assemblies consisting of few 10–100s of lipid molecules. These dynamics occur over length scales of few tens to few 100 Å and over time scales of sub-ns to few hundred ns (see **Figure 1**), referred to here as mesoscopic scales. It is indeed on these scales that key biological activity takes place at the membrane level[17]. This includes viral budding[18], channel gating[19], and membrane-protein interactions[20]. It is also important to point out that the energy landscape of membrane proteins[21,22] shows that conformational changes in proteins – necessary for their regulatory role – happen over the ns time scales[23] of collective membrane fluctuations, further emphasizing the importance of mesoscopic dynamics in the biological function of cell membranes and their bioinspired analogs[20]. This paper focuses on the two primary mesoscopic dynamic modes in lipid membranes, namely, bending fluctuations and thickness fluctuations.

The main challenge in directly probing these fluctuation modes is the difficulty in simultaneously accessing their spatial and temporal scales using standard spectroscopy methods. The other challenge is that direct contact techniques could impact the same fluctuations they are meant to measure[16]. This is further exacerbated by the compositional and structural complexity of biological membranes[24,25], which results in non-homogeneous membrane features, including lipid domain formation[26–30] and membrane asymmetry[31–33] – demanding selective probes to understand the dynamics of different membrane features. Fortunately, these challenges can be overcome with non-invasive neutron spectroscopy methods, such as neutron spin echo (NSE), which inherently access the required length and time scales, and further enable studies of selective membrane features without changing their physicochemical environment[34]. Indeed, over the last few years NSE spectroscopy has evolved into a unique and powerful probe of collective membrane dynamics[35]. Results from NSE studies on lipid membranes have produced new insights into mechanical[36,37] and viscoelastic[38,39] properties of lipid membranes and have shed new light on their potential role in biological function[40,41].

The NSE spectroscopy technique is based on an interferometric instrument design, first proposed by Mezei[42], using a series of spin-flippers and magnetic coils to control the precession of the neutron spin as neutrons traverse the instrument. The design rests on magnetic mirroring of the magnetic field elements with respect to the sample position (**Figure 1A**). This implies that in the absence of energy exchange between the neutron and the sample, the neutron performs the same number of spin precessions, in opposite directions, in the first and second half of the instrument (notice the π-flipper between the two precession coils). As a result, the final spin state of the neutron remains unchanged relative to the initial state – a phenomenon referred to as spin-echo (see transparent neutron in **Figure 1A**). However, when the neutron energetically interacts with the sample, the energy exchange modifies the number of spin precessions in the second half of the instrument, leading to a different final spin state (see **Figure 1A**). This is experimentally detected as a loss in polarization, as will be shown later in this paper. For more details on the NSE technique, the reader is referred to dedicated technical papers[42–45].

Here, a simplified description is presented to provide a rough estimate of the length and time scales accessible with NSE. The length scales are determined by the range of achievable wavevector transfers, $Q = 4\pi \sin\theta/\lambda$, where 2θ is the scattering angle and λ is the neutron wavelength. One can see that q is set by the wavelength range and the extent of rotation of the second arm of the spectrometer (see **Figure 1A**). A typical q-range on NSE spectrometers is ~0.02––2 Å^{-1} [46,47], and up to 0.01–4 Å^{-1} with recent upgrades[48,49], corresponding to spatial scales of ~1–600 Å. On the other hand, the accessible time scale is calculated from the total precession angle (or phase) acquired by the neutron within the magnetic precession coils, and is found to be[50]: $\varphi_{\mathrm{tot}} \cong \gamma B l \hbar\omega \,/\, m_n v^3 \equiv \omega t$. In this expression, t is the Fourier time defined as $t = \gamma B l \hbar \,/\, m_n v^3 = 0.186\, B l \lambda^3$, where γ is the neutron gyromagnetic ratio, l is the coil length, and B is the strength of the coil's magnetic field. It is worth pointing out that the Fourier time is a quantity that is strictly dependent on the instrument geometry, magnetic field strength, and neutron wavelength. For instance, using neutrons of wavelength $\lambda = 8\ \text{Å}$ and instrument settings of $l = 1.2\ \mathrm{m}$ and $B = 0.4\ \mathrm{T}$, the Fourier time is calculated to be $t \sim 50\ \mathrm{ns}$. Experimentally, the Fourier time is tuned by changing the current in the precession coils (i.e., magnetic field strength) or using different neutron wavelengths, resulting in typical NSE time scales of ~ 1 ps to 100 ns. However, recent upgrades in NSE spectrometers have enabled access to longer Fourier times, up to ~400 ns on the J-NSE-Phoenix spectrometer at the Heinz Maier-Leibnitz Zentrum[51] and the SNS-NSE spectrometer at Oak Ridge National Lab[48], and up to ~1,000 ns at the IN15 NSE spectrometer at the Institut Laue-Langevin (ILL)[49].

Besides direct access to the length and time scale of membrane dynamics, NSE has the inherent capabilities of neutron isotope sensitivity[52]. Specifically, the ability of neutrons to interact differently with the isotopes of hydrogen, the most abundant element in biological systems, results in a different neutron scattering length density,[34] or NSLD (the equivalent of the optical index of refraction[50]), when protium is substituted by deuterium. This enables an approach known as contrast variation, which is commonly used to highlight specific membrane features or conceal others – the latter scenario is referred to as contrast matching. A frequent application of contrast variation/matching is the substitution of water (NSLD = $-0.56 \times 10^{-6}\ \text{Å}^{-2}$) by heavy

water or D_2O (NSLD = 6.4×10^{-6} Å^{-2}) to amplify the neutron signal from protiated lipid membranes (NSLD $\sim 2 \times 10^{-6}$ Å^{-2}). This approach is highly effective in studies of membrane structure because the penetration of D_2O into the headgroup region of the membrane allows accurate determination of the membrane thicknesses (see **Figure 2A**, left panel) and of the location of different lipid subgroups when more sophisticated models are applied[53,54]. This paper highlights some examples on the use of contrast variation for studies of collective dynamics in biomimetic membranes and select membrane features.

The effectiveness of NSE in providing unique insights into dynamical and functional membrane properties is illustrated through tangible examples of NSE studies on model and biologically relevant lipid membrane systems with emphasis on mesoscale dynamics in free-standing membranes, in the form of liposomal suspensions. For NSE measurements of in-plane membrane dynamics, the reader is referred to dedicated publications on grazing-incidence neutron spin-echo spectroscopy (GINSES)[55,56] and other studies of aligned multilamellar membrane stacks[57–60].

For simplicity, this paper highlights three different schemes of membrane deuteration illustrated on a well-studied domain-forming, or phase separating, lipid bilayer system of 1,2-dimyristoyl-sn-glycero-3-phosphocholine (DMPC) and 1,2-distearoyl-sn-glycero-3-phosphocholine (DSPC) mixtures[61,62]. The two lipids are characterized by a length mismatch in their hydrocarbon tails (14 carbons/tail in DMPC vs 18 carbons/tail in DSPC) and different melting temperatures ($T_{m,\,DMPC}$ = 23 °C vs $T_{m,\,DSPC}$ = 55 °C). This results in lateral phase-separation in DMPC:DSPC membranes at temperatures between the upper and lower transition temperatures of the mixture[63]. The deuteration schemes considered here are chosen to demonstrate the different dynamic modes accessible in NSE measurements on liposomal membranes, namely, bending fluctuations, thickness fluctuations, and selective bending/thickness fluctuations of lateral domains. All lipid compositions are reported for DMPC:DSPC bilayers prepared at a mole fraction of 70:30, using commercially available protiated and perdeuterated variants of DMPC and DSPC. All sample descriptions are based on 4 mL of liposomal suspension, in D_2O, with a lipid concentration of 50 mg/mL, for a total lipid mass of $M_{\mathrm{tot}} = 200$ mg per sample.

PROTOCOL:

1. Deuteration scheme required for the experiment

1.1. For bending fluctuation measurements, make fully protiated liposomes in D_2O (D 99.9%) or D_2O-buffer (e.g., phosphate buffer prepared with D_2O instead of H_2O). Use fully protiated DMPC ($C_{36}H_{72}NO_8P$) and DSPC ($C_{44}H_{88}NO_8P$) with $m_{\mathrm{DMPC}} = M_{\mathrm{tot}} \frac{X_{\mathrm{DMPC}} M\mathrm{w}_{\mathrm{DMPC}}}{X_{\mathrm{DMPC}} M\mathrm{w}_{\mathrm{DMPC}} + X_{\mathrm{DSPC}} M\mathrm{w}_{\mathrm{DSPC}}} =$ 133.4 mg, where X_{DMPC} and X_{DSPC} are the mole fractions of DMPC and DSPC, here set to 0.7 and 0.3, respectively, and $\mathrm{Mw}_{\mathrm{DMPC}}$ and $\mathrm{Mw}_{\mathrm{DSPC}}$ are the molar weights given by 677.9 g/mol and 790.1 g/mol, respectively. Similarly, $m_{\mathrm{DSPC}} = 66.6$ mg. This deuteration scheme increases the scattering contrast between the membrane (NSLD $\sim 2 \times 10^{-6}$ Å^{-2}) and the deuterated buffer (NSLD $\sim 6.4 \times 10^{-6}$ Å^{-2}) and amplifies the signal from membrane undulations (see **Figure 2A** left panel).

1.2. To measure the bending dynamics of select lateral membrane features, e.g., matrix dynamics in phase-separating DMPC:DSPC membranes, use protiated DMPC ($C_{36}H_{72}NO_8P$) and deuterated, DSPC-d83 ($C_{44}H_5NO_8PD_{83}$, $Mw = 873.7$ g/mol), such that $m_{\mathrm{DMPC}} = 128.8$ mg and $m_{\mathrm{DSPC-d83}} = 71.2$ mg. This deuteration scheme minimizes the scattering from the undesired DSPC-rich domains, enabling selective measurements of bending fluctuations from the DMPC-rich matrix (see **Figure 2B** middle).

NOTE: To find the optimal lipid deuteration required for a specific contrast matching scheme, utilize available web-based scattering length density (SLD) calculators, such as the one developed by the NIST Center for Neutron Research[64]. These web-based interfaces are equipped with user-friendly tools for easy calculation of the SLD of lipids with various degrees of deuteration, as well as that of lipid mixtures.

1.3. For NSE measurements of average membrane thickness fluctuations (with no lateral contrast), use tail-deuterated variants of the constituent lipids, i.e., DMPC-d54 ($C_{36}H_{18}NO_8PD_{54}$, $\mathrm{Mw} = 732.3$ g/mol) and DSPC-d70 ($C_{44}H_{18}NO_8PD_{70}$, $\mathrm{Mw} = 860.1$ g/mol)[35,38], such that $m_{\mathrm{DMPC-d54}} = 133.0$ mg and $m_{\mathrm{DSPC-d70}} = 67.0$ mg. This contrast scheme (**Figure 2A**, right panel) amplifies the scattering signal from the lipid headgroups (NSLD $\sim 4.5 \times 10^{-6}$ Å^{-2}) by contrast-matching the tail-group (NSLD $\sim 6.4 \times 10^{-6}$ Å^{-2}) to the deuterated buffer enabling the detection of fluctuations in membrane thickness.

1.4. For thickness fluctuation studies of select membrane compartments, e.g., DMPC-rich matrix, use the same strategy described in step 1.2 by substituting protiated DMPC lipids with their tail-deuterated analogs, i.e., DMPC-d54, such that the DSPC-rich domains are contrast-matched to the deuterated buffer and the primary scattering signal is from the headgroup region of the tail-deuterated DMPC-rich matrix.

2. Preparation of lipid suspension for extrusion

2.1. Calculate the mass of each constituent in the sample, depending on sample composition. As a rule of thumb, for samples with multiple molecular components, the mass of a component i is given by its molar mass, Mw_i, weighted by its mole fraction, X_i, and normalized over all components such that: $m_i = M_{\mathrm{tot}} \frac{X_i \mathrm{Mw}_i}{\sum_i X_i \mathrm{Mw}_i}$ where $\mathrm{M}_{\mathrm{tot}}$ is the total mass, set here to 200 mg. See the example above for DMPC-DSPC lipid bilayers with different deuteration schemes. Add a small amount of charged lipid (up to 4 mol%), when possible, to reduce liposomal multilamellarity[65].

2.2. Using a digital semi-microbalance, weigh the calculated masses of lipids (and other sample constituents, e.g., proteins, nanoparticles, etc.) and add them to a vial or round-bottom flask – remember to weigh the vial or flask beforehand. Add 1 mL of solvent to dissolve the weighed components by manually mixing inside a hood. For pure lipid samples, use chloroform or ethanol. For samples with additional, non-lipid components (e.g., nanoparticles), choose a common solvent that disperses all components.

2.2.1. For small lipid amounts (<10 mg), prepare a stock solution and pipette the required volume into the mixture.

NOTE: Do not add excessive amounts of solvent as it will significantly slow down the solvent drying step described below.

2.3. Dry the lipid solution, inside a hood, by gently streaming an inert gas (e.g., nitrogen, argon) in the vial while slowly rotating the vial at an angle. Keep the vials in tilted position to create a thin film of dried lipid on the vial walls, which will allow for even drying. Intermittently place the vial in a water bath at 35 °C to circumvent evaporation-mediated cooling, which will slow down the evaporation.

2.4. Place the vials overnight in a vacuum oven at ~35 °C to fully remove the residual solvent. For unsaturated lipids, purge vacuum with an inert gas to minimize oxidation.

2.5. To ensure full solvent removal, weigh the vial after lipid drying and confirm that there is no excess mass beyond the measured amounts of materials. Do this by subtracting the mass of the vial from the measured mass after drying. If there is excess mass, dry the sample under vacuum for another 6 h. Repeat this process as needed.

2.6. Hydrate the lipid film with 4 mL of D_2O or D_2O-buffer to obtain a lipid concentration of 50 mg/mL. For lipids with high transition temperatures, such as DMPC-DSPC mixtures, heat the buffer to above the transition temperature (60 °C) to ensure even mixing.

NOTE: Since NSE experiments require relatively large sample volumes (~4 mL), consider hydrating the sample using half of the required buffer, i.e., 2 mL, to minimize the number of extrusions per sample (see section 3). In this case, add the remaining half of the buffer post extrusion. Notice that the capacity of syringes used in extrusion is limited to 1 mL. Thus, hydrating with 4 mL of buffer would require four sets of extrusion.

2.7. Vortex-mix the hydrated lipid solution until the lipid film is fully dissolved and is no longer visible on the walls of the vial. At this stage, the hydrated lipids form multilamellar vesicles and micron sized multilamellar stacks and the suspension appears milky white.

2.8. To facilitate the breaking of the lipid stacks and to reduce multilamellarity, perform five freeze/thaw cycles by placing the vial of hydrated lipid solution in a lab grade freezer (preferably -80 °C freezer) until fully frozen and then transferring the vial to a 35 °C water bath until the lipid solution is fully thawed. Vortex the thawed solution until homogenous. Repeat four more times.

NOTE: Alternatively, a dry ice bath can be made for freeze thawing by combining acetone and dry ice.

3. Extrusion of the hydrated lipid solution

3.1. Assemble the extruder setup using a polycarbonate membrane between two membrane supports and adding two paper filters on each side to provide additional support. Use a polycarbonate membrane with a pore size that matches the target liposomal size (common pore sizes for NSE experiments are 50 nm and 100 nm – typically, 100 nm-diameter liposomes allow for less constrained membrane fluctuations, but smaller 50 nm liposomes could be used for curvature studies). Ensure that the polycarbonate membrane is fully stretched before completing the assembly and tightening the external extruder casing.

3.2. Hydrate the polycarbonate membrane by passing ~0.3 mL of D_2O or D_2O-buffer a few times through the membrane assembly using airtight glass syringes. Utilize the same buffer used in sample preparation. Leave it for at least 10 min, then completely suck the buffer out before introducing the sample.

3.3. Fill a 1 mL gas-tight syringe with the prepared lipid solution and insert into one end of the extruder apparatus. Then, insert an empty syringe into the opposite end. Once the syringes are connected to the extruder assembly, place it into the extruder block.

3.4. If elevated temperatures are needed for extrusion, as in the case of saturated lipids with high transition temperatures (e.g., DSPC, T_m = 55 °C), preheat the extruder heating block above the lipid transition temperature (e.g., 60 °C), by placing the heating block on a hot plate or by using a circulation bath as shown in **Figure 3A**.

NOTE: This step is crucial to ensure homogeneous mixing of lipids and to avoid exerting extreme pressure during extrusion, which could rupture the polycarbonate membrane. For lipid samples with low transition temperatures (<25 °C), perform the extrusion at room temperature.

3.5. To extrude the lipid solution, attach the extruder set to a programmable syringe pump with an aluminum/steel frame as shown in **Figure 3A**. For temperature-controlled extrusions, add a custom-built extruder base with a fluid channel and attach to a circulating water bath.

3.6. Program the syringe pump to perform 15–20 extrusion cycles following the manufacturer's manual. When extruded, the color of the lipid solution changes from milky white to transparent opal blue (**Figure 3B,C**), indicating a final liposomal size that is smaller than the wavelength of visible light – as expected. For the type of syringe pump shown in **Figure 3A**, follow the steps below.

3.6.1. Start by adjusting the pump settings. Hold down the **Rate** button and enter the extrusion rate (50.99 mL/h), then press the **Diameter** button and enter the syringe diameter (4.606 mm). Use the up arrows under each digit on the screen to change that digit value.

3.6.2. Place the extruder set with the sample syringe to the right (see **Figure 3A**). Press the **Withdraw** button until the withdraw light turns on. Press **Start** and wait for the sample to dispense into the left (empty) syringe.

3.6.3. Hit the **Stop** button just before the sample (right) syringe is fully empty. Record the dispensed volume and use it to program the extrusion cycle. Hold down the **Rate** button until phase 1 (PH:01) appears on the screen. Press the **Volume** button to enter the dispensed volume recorded earlier. In this phase, make sure that the Withdraw light is off – this dispenses the sample in the right direction.

3.6.4. Press the **Rate** button again and use the rightmost up arrow to access phase 2 (PH:02). Press **Volume** to enter the same value of the dispensed volume recorded earlier. In this phase, press the **Withdraw** button until the Withdraw light is on – this dispenses the sample to the left.

3.6.5. To repeat this cycle, press the **Rate** button again and use the rightmost up arrow to access phase 3 (PH:03). Press the **Volume** button until LP:SE appears on the screen and set it to 20. This is the number of loops or repeats that the pump will perform. Finally, press the **Rate** button, access phase 4 (PH:04), and hit the **Volume** button to get to the **Stop** function. The pump is now set up for automated extrusion.

3.6.6. Press **Start** to start the extrusion cycle.

3.7. Empty the syringe containing the extruded lipid suspension in a clean vial and prepare for storage or measurements. For lipid samples with high melting temperature, store the sample above the fluid phase transition until measured. Otherwise, keep samples at room temperature.

3.8. If the lipid suspension is to be stored for an extended period, store the samples at 4 °C. Do not freeze extruded samples as freezing will cause the vesicles to burst (the suspension will turn milky white again).

4. NSE measurements for the sample(s) and reduction of the collected data

4.1. Prior to the NSE experiment, characterize the extruded liposomal sample from step 3.7 using available methods to ensure adequate sample quality. A list of potential charcaterization methods that can be used to assess the quality of liposomal suspensions for NSE experiments, e.g., size distribution, multilamellarity, lateral membrane structure, is included in the discussion section.

4.2. Determine the Q-range and corresponding instrument settings required for the experiment. For bending rigidity measurements of lipid bilayers, use a Q-range of $\sim (0.04 - 0.2)$ Å^{-1}. For studies of membrane thickness fluctuations, use a Q-range of $\sim (0.04 - 0.1)$ Å^{-1} corresponding to the membrane thickness[35,66,67].

NOTE: Discuss the experimental setup with the instrument scientist before the start of the experiment. As mentioned earlier, SANS characterization of the sample is necessary, especially if prior information of the scattering signal is not available as in selectively deuterated membranes.

Alternatively, run static (also known as diffraction) measurements over a limited Q-range on the NSE instrument, with the caveat that such measurements take much longer compared to SANS.

4.3. Using a syringe or a transfer pipette, load the extruded liposomal suspension(s) in the designated sample cells available at NSE beamlines. Note that standard NSE sample cells come in thicknesses of 1, 2, 3, and 4 mm. Choose the cell thickness in such a way to optimize the scattering signal while keeping the incoherent background signal to a reasonable intensity.

NOTE: As a rule of thumb, use sample cells with 1 or 2 mm pathlength for protiated liposomes in deuterated buffer – thicker cells could result in multiple scattering effects that are difficult to correct for. For liposomes with higher levels of deuterations (e.g., tail contrast-matched liposomes or asymemetric liposomes with single protiated leaflets), consider using a thicker sample cell (e.g., 3 or 4 mm pathlength) to enhance the counting statistics if the sample is available in larger quantities – sometimes this can be cost prohibitive.

4.4. Prepare an identical sample cell for the buffer. Use the same buffer as in the liposomal suspension. Measurements on the buffer are necessary for intensity normalization and background (BKG) corrections.

4.5. Place the sample cell(s) in the sample holder of the NSE spectrometer, program the measurement runs, and collect echo data. Consult with the instrument scientist about programming the measurements if a first-time NSE user.

4.6. Perform two additional sets of measurements needed for the data reduction: Resolution (*R*) and transmission (*T*) measurements.

4.6.1. Perform Resolution (*R*) measurement on an elastic scattering reference (e.g., carbon) – to be run under the same settings; i.e. same wavevector and Fourier times as the sample and buffer measurements.

4.6.2. Perform transmission (*T*) measurements on the sample and buffer to calculate the intensity of the transmitted neutron beam (see step 4.9. below). The transmission is calculated as the the ratio of neutron counts from the sample or buffer divided by the neutron counts for an open beam (i.e., with an empty sample position).

4.7. Use the dedicated data reduction software for the NSE spectrometer on which the measurements are performed to reduce the collected data.

NOTE: Different spectrometers might utilize different software or user interfaces. Below is an example of NSE data reduction using the Data Analysis and Visualization Environment (DAVE)[68] software specifically written for the NSE spectrometer at the NIST Center for Neutron Research.

4.7.1. Open the DAVE software and select **Reduce NSE Data** from the data reduction menu. Several pop-up windows will appear.

4.7.2. Upload the data files over different Q-values using the Open .echo Files from the file menu. These files correspond to the raw data files with the spin echo signals and have the extension .echo in the file name. Once the file upload is complete, the files will show under the available data sets.

4.7.3. Right-click on the selected file and label it according to the measurement it corresponds to; i.e., Sample, Cell (for empty cell or buffer), or Resolution.

4.7.4. Group the detector pixles in 2 x 2 to improve the signal-to-noise ratio using the **Data Set** tab. Apply the same binning to all files; i.e., Resolution, Cell, and Sample.

4.7.5. Inspect the data over all pixel groups and mask those with poor signals (see **Figure 4B**) by pressing the **m** key on the keyboard. Press **Enter** to access a pop up window to apply the same mask to all Fourier times or subsequent Fourier times. This can also be applied to individual pixels at any point during data reduction. Masked pixels will turn green.

4.7.6. Ensure that the collected data is in the form of an echo signal, i.e., cosine function in terms of the phase current, over each detector pixel (see **Figure 4A**).

NOTE: The phase current is proportional to the precession angle of the neutron spin; hence, it is common to represent the phase current as a phase angle as shown in **Figure 4A**. For measurements on pulsed sources, additional time of flight calculations are applied to the data to obtain the echo signals as a function of incident neutron wavelength within a neutron pulse.

4.7.7. Start by fitting the resolution file. Select a resolution file from the uploaded file list and right-click on the file. Select **Fit Operations: Fit Echoes (Resolution)** from the pop-up menu.

4.7.8. Ensure that the fits of the echo signals yield a number of fitting parameters, including the parameter, A, required in step 4.8. The fits are automatically performed using following expression.

$$N = N_0 + A \exp\left[\frac{(\phi_c - \phi_0)^2}{2\sigma^2}\right] \cos\left[\frac{360}{\zeta}(\phi_c - \phi_0)\right] \qquad (1)$$

Here, ζ is the period of the echo signal (i.e., cosine function in **Figure 4A**), σ is the width of the Gaussian envelope determined by the mean wavelength and wavelength spread of the incident neutron beam, ϕ_c is the phase current, and ϕ_0 is the echo point which depends on the field path experienced by neutrons[50]. Physical information about the sample is encoded in the amplitude, A, of the cosine function in equation (1).

NOTE: The width of the Gaussian envelope is based on values predetermined by the instrument scientist and should not be changed. The other paramters are variables that are fitted to the specific echo signal over each pixel.

4.7.9. Inspect the fit results by clicking on each pixel to show the resulting fitting parameters, the quality of the fit, and the mean square deviation of the fit. To inspect the error associated with each fitting parameter over the entire detector, select **Image Options** and then select the fitting parameter of interest. This will generate a map with the value of the fitting paramter over each pixel. Right-click on the detector image. A pop up window will appear showing an error bar map of the selected fitting parameter.

4.7.10. If the fit over a specific pixel is unsatisfactory (e.g., fit parameeters with large error bars), refit the signal over that specific pixel. Select that **pixel**, press the **Fitting** tab, and then press **Fit Pixel**. Input new starting parameters for the phase (ϕ_0) and period (ζ) in the **Fitting** tab to obtain a more satisfactory fit.

NOTE: It is useful to plot the fitted phase as a function of Fourier Time. To do so, go to the main plot window and select **Fit Phase v. Fourier Time**. This plot should be smooth and continuous. Inspect discontinuities in this plot and refit the pixels that they correspond to.

4.8. Reduce the Sample or Cell file by selecting the corresponding file from the uploaded and labeled file list.

4.8.1. Inspect all pixels and mask the ones with bad statistics as described in step 4.7.5.

4.8.2. Right-click on the file and select **Fit Operations: Import Phases (Sample, Cell)**. This imports the phases and the applied mask from the Resolution file.

4.8.3. Fit the echo signals using the same procedure described before for the Resolution file (steps 4.7.8–4.7.10). In fitting the Sample and Cell files, do not change the values of the period and echo phase point imported from the Resolution fits. These parameters depend on the instrumental settings and should not vary with samples.

4.8.4. Before proceeding to data reduction, input the beam center for all data files. Select the data file, go to the **General** tab and enter X and Y beam center values. These values are recorded during the experiment.

4.8.5. Once the fits to the Sample, Cell, and Resolution files are complete, calculate the normalized intermediate scattering function to be used later in data analysis and interpretation. To do that, right click on the Sample file to be reduced from the list of fitted files, and select **Calculate I(Q)** from the pop up menu. A window will appear with entry choices for the Resolution and Cell (i.e., buffer) files, and the number of Q-arcs (see step 4.9). After entering all the required informaiton, press the **OK** button. The results will appear in a new window.

NOTE: The data reduction is performed according to the following equation to obtain the normalized intermediate scattering function[69].

$$\frac{S(\tilde{Q},t)}{S(\tilde{Q},0)} = \frac{\left[\frac{2(A-(T^{BKG}/T)\,A^{BKG})}{(N_{up}-N_{down})-(T^{BKG}/T)\,(N_{up}^{BKG}-N_{down}^{BKG})}\right]}{\frac{2A^{R}}{N_{up}^{R}-N_{down}^{R}}} \quad (2)$$

where t is Fourier time, N_{up} and N_{down} are the neutron counts in the non-spin-flip and spin-flip configurations (measured with the π/2-flippers off and the π-flipper off and on, respectively), and the superscripts, *BKG* and *R*, correspond to the background and resolution measurements, respectively, as defined in steps 4.4 and 4.6. Note that the beam polarization $\propto S(\tilde{Q},t)/S(\tilde{Q},0) \propto 2A/(N_{up}-N_{down})$, thus changes in the spin state due to energy exchange between the neutron and the sample is detected as a drop in the polarization (from unity).

4.9. Finally, group the detector pixels into *Q*-arcs as shown in **Figure 4B** to obtain the *Q*-dependence of the normalized intermediate scattering function, $S(Q,t)/S(Q,0)$. This is technically referred to as data binning and should be done judiciously, i.e., taking into account the counting statistics from the sample and the expected standard deviation of the data over the grouped pixels.

4.10. For strongly scattering samples, divide the detector into more Q-arcs while maintaining reasonable error bars on the resultant intermediate scattering function, $S(Q,t)/S(Q,0)$. This yields more Q data points and is important for the data analysis procedure described below. Be aware that for weakly scattering samples, excessive binning results in poor decay signals, i.e., large error bars on $S(Q,t)/S(Q,0)$, could result in large uncertainties in the data fits and the extracted fit parameters.

5. Data analysis and interpretation

5.1. Fit the normalized intermediate scattering functions, $S(Q,t)/S(Q,0)$, obtained from the data reduction above to a stretched exponential function with a stretching exponent of 2/3[70].

$$S(Q,t)/S(Q,0) = \exp[-(\Gamma(Q).t)^{2/3}], \quad (3)$$

NOTE: An example of these fits is provided in **Figure 5B**. Fits of $S(Q,t)/S(Q,0)$ to equation (3) yield the Q-dependent relaxation rates $\Gamma(Q)$.

5.2. Plot $\Gamma(Q)$ as a function of Q and fit to a suitable model to extract relevant membrane parameters.

REPRESENTATIVE RESULTS:

NSE studies accessing bending fluctuations are typically performed over a Q-range of $\sim (0.04 - 0.2)$ Å^{-1}. This Q-range corresponds to intermediate length scales between the membrane thickness and the liposomal radius, where bending dynamics dominate. Measurement over an extended Q-range can give access to additional dynamic modes, including liposomal diffusion and

intramembrane dynamics. For more details on the cross-over in membrane dynamics accessed by NSE, check these relevant publications[25,71]. It is important to emphasize that NSE signals are proportional to: $I_{\mathrm{coh}}(Q,t) - \frac{1}{3} I_{\mathrm{inc}}(Q,t)$, where I_{coh} and I_{inc} are, respectively, the coherent and incoherent scattering intensity from the sample. Therefore, it is advisable to prepare NSE liposomal samples in deuterated buffers (i.e., buffers prepared with D_2O instead of H_2O) to minimize the incoherent scattering signal, mainly contributed by the hydrogen content of the sample. However, in some cases intermediate deuteration schemes (i.e., using mixtures of D_2O and H_2O) might be necessary to obtain optimal contrast conditions. Typically, NSE measurements of membrane bending fluctuations are performed on fully protiated liposomes in deuterated buffer, referred to as fully contrasted liposomes in **Figure 5**. This deuteration scheme results in a large SLD difference between the membrane core ($\sim 2 \times 10^{-6}\ \text{Å}^{-2}$) and its deuterated fluid environment ($\sim 6.4 \times 10^{-6}\ \text{Å}^{-2}$), which significantly enhances the scattering signal from the liposomal membranes and improves the measurement statistics of bending dynamics. This contrast scheme (**Figure 2A** left panel) is frequently utilized in studies of bending rigidity of lipid membranes with single[38,72] and multiple[39,66] lipid components and in studies of membrane softening/stiffening by biological inclusions (e.g., cholesterol, drug molecules, peptides/proteins)[36,37,73–75], and synthetic additives (e.g., nanoparticles)[76,77].

Measurements of bending fluctuations result in relaxation rates that follow a q^3 dependence, as predicted by Zilman and Granek for thermally undulating elastic thin sheets[70]. A refined form of this q-dependence is obtained from theoretical corrections by Watson and Brown[78], which take into account the effects of intermonolayer friction proposed by Seifert and Langer[79]. By additionally defining the neutral plane to be at the interface between the hydrophilic headgroups and the hydrophobic tails of the membrane, the bending relaxation rates can then be fitted to the following expression[38].

$$\Gamma_{\mathrm{bend}}(Q) = 0.0069\ \frac{k_{\mathrm{B}}T}{\eta_{\mathrm{buff}}} \sqrt{\frac{k_{\mathrm{B}}T}{\kappa}}\ Q^3, \qquad (4)$$

where η_{buff} is the buffer viscosity, $k_{\mathrm{B}}T$ is the thermal energy, and κ is the bending rigidity of the measured membrane (or of the contrasted portion of the membrane in selectively deuterated systems). This type of measurement enables direct calculation of membrane elastic properties in the form of the bending rigidity modulus. Note that κ is extracted from the slope of the linear fit of $\Gamma\ vs.\ Q^3$, as shown in **Figure 5C**.

On the other hand, NSE measurements of membrane thickness fluctuations show deviations from the Q^3-dependence in $\Gamma(Q)$ around Q values that correspond to the membrane thickness (see **Figure 2** in ref.[66]). To isolate the thickness fluctuation signal, one can divide $\Gamma(Q)$ by Q^3, as shown in **Figure 5D**. The resulting data shows that the excess dynamics due to thickness fluctuations follow a Lorentzian function in Q, as recently corroborated in coarse-grained molecular dynamics (MD) simulations[67]. To fit the observed excess dynamics, Nagao et al.[38] developed an expression based on the theoretical framework of membrane fluctuations by Bingham et al.[80] as follows.

$$\frac{\Gamma}{Q^3} = \frac{\Gamma_{\mathrm{bend}}}{Q^3} + \frac{K_{\mathrm{A}} k_{\mathrm{B}} T}{\mu Q_0^3 k_{\mathrm{B}} T + 4\mu q_0 K_{\mathrm{A}} A_{\mathrm{L}} (Q - Q_0)^2}, \qquad (Eq. 5)$$

In this expression, Q_0 is the peak *Q*-value corresponding to the membrane thickness (which can be independently obtained from SANS measurements), μ is the in-plane membrane viscosity, A_{L} is the area per lipid (measured with SANS/SAXS), and K_{A} is the area compressibility modulus. Assuming that K_{A} can be calculated from κ using the polymer brush model, this expression reduces to one fit parameter, namely, the membrane viscosity μ, presenting a new approach to measure membrane viscosity without the need for fluorescence labeling or particle tethering/tracking[13]. The premise is that according to deformation models of elastic thin sheets[81], κ and K_{A} are interdependent such that: $\kappa = K_{\mathrm{A}} t_{\mathrm{m}}^2/\beta$, where t_{m} is the mechanical (or deformable) membrane thickness and β is a constant that describes interleaflet coupling. The assumption is that β = 12 for fully coupled leaflets, β = 48 for completely uncoupled leaflets, and β = 24 for intermediately coupled leaflets. The latter is referred to as the polymer brush model[81] and has been shown to apply in single-component and binary fluid lipid membranes[39]. However, this needs to be approached with caution. For instance, recent simulations by Doktorova et al.[82] showed that for the polymer brush model to hold in unsaturated lipid membranes containing cholesterol, a modified expression of the mechanical membrane thickness must be used. Ideally, if an independent measurement of K_{A} is possible, e.g., using micropipette aspiration[83], then combining K_{A} results with NSE bending rigidity measurements would present a unique opportunity to investigate interleaflet coupling in model and biological membranes – a long standing question in membrane biophysics and structural biology. Once the values of K_{A} are validated, they can be used in equation 5 to obtain the mesoscopic membrane viscosity.

FIGURE LEGENDS:

Figure 1: NSE instrument design and synergistic overlap with length/times scales of mesoscopic membrane dynamics. (**A**) Schematic of the different magnetic elements of an NSE instrument, used to manipulate the spin of neutrons traversing the instrument from left to right. The highlighted neutron indicates change in spin orientation (or polarization loss) due to energy exchange between the neutron and the sample, whereas the transparent neutron represents spin-echo, i.e., no change in the neutron spin due to zero energy exchange. The grey arrow indicates the possibility of rotating the second arm of the spectrometer to access larger scattering angles. (**B**) Pictorial representation of hierarchical dynamics in lipid membranes, showing various dynamic modes that span multiple length and time scales. The shaded area represents the length and time scales accessed by NSE, which overlap with the mesoscales of collective membrane fluctuations, namely, bending and thickness fluctuations.

Figure 2: Examples of possible deuteration schemes in NSE experiments on lipid membranes. (**A**) Left: Fully contrasted membranes, e.g., protiated membranes in deuterated buffer, showing the NSLD profile along the normal to the membrane surface. The difference in the NSLD between the headgroup (~ 2×10^{-6} Å^{-2}) and tail region (~ 4.5×10^{-6} Å^{-2}) of the membrane is due to the headgroup hydration with deuterated buffer. Right: Tail-contrast matched membranes such

that the hydrocarbon tail region of the membrane has the same NSLD as the buffer, as shown in the corresponding NSLD profile along the membrane normal. (**B**) Domain-forming membranes with two neutron contrast schemes where the domains (center) or the matrix (left) are contrast-matched to the buffer, enabling selective studies of matrix or domain dynamics, respectively. This figure has been modified from Nickels et al., JACS 2015[41]. (**C**) Asymmetric membranes prepared by cyclodextrin exchange between protiated and deuterated lipid vesicles, resulting in the deuteration of one membrane leaflet while keeping the other leaflet protiated. This allows studies of the bending dynamics of the protiated leaflet and provides insights into the mechanical coupling between opposing leaflets in asymmetric membranes. This figure has been modified from Rickeard et al., Nanoscale 2020[40].

Figure 3: Illustration of the setup for automated extrusion of liposomes. (**A**) Custom-built automated extruder using a syringe pump, a mini extruder set, and an aluminum/steel frame to enable cyclic extrusions. (**B**) and (**C**) show the difference in visual appearance of lipid suspensions before (milky white) and after (transparent opal blue) extrusion. This is due to the initial formation of micron-sized lipid stacks or giant vesicles which are on the order of, or larger than, the wavelength of visible light. After extrusion, the suspension will comprise nanoscopic vesicles (~100 nm), which are smaller than the wavelength of visible light, yielding a transparent suspension.

Figure 4: Representative data from NSE experiments on liposomal suspensions. (**A**) Example of an echo-signal over a single detector pixel (marked pixel in panel B), showing the fits of the echo signal using equation (1), with an illustration of the different parameters required in the echo fit. Note that the echo signal is plotted as a function of the phase angle instead of the phase current as discussed in step 4.7 of the protocol. (**B**) NSE detector image showing the variation in neutron counts per pixel. The image also shows eliminated detector pixels (green) due to poor echo signals. The binning of the detector pixels in Q-arcs (also known as Debye-Scherrer rings) yields the q-dependence of the intermediate scattering function, needed for analyzing and interpreting NSE data. This figure was modified from Ashkar, J. Appl. Phys. 2020[50].

Figure 5: Representative results from NSE experiments on liposomal suspensions with different deuteration schemes. (**A**) Scattering geometry of a neutron interacting with a liposome, showing the scattering angle, 2θ, and the wavevector transfer, $\vec{Q}$. (**B**) Intermediate scattering functions, $S(Q,t)/S(Q,0)$, exhibit decays as a function of the Fourier time. Fit of the measured decays to a stretched exponential function given by equation 3 yields the relaxation rates, $\Gamma(Q)$. (**C**) For fully protiated liposomes in deuterated buffer, $\Gamma(Q)$ follows a Q^3 dependence, typical of bending dynamics. The linear fit of the obtained data to a Zilman-Granek model yields the bending rigidity modulus of the membrane. (**D**) For tail deuterated liposomes, excess dynamics are observed in addition to bending fluctuations and are most pronounced at Q-values that correspond to the membrane thickness. Fitting the excess dynamics to a Lorentzian function (equation 5) allows extraction of the membrane viscosity. Data sets were collected on the NSE spectrometer at NIST.

DISCUSSION:

NSE is a powerful and unique technique in measuring mesoscopic dynamics of lipid membranes under various conditions. The effective utilization of NSE depends on sample quality, neutron contrast, and the range of accessible dynamics that can be probed for a given sample. Thus, several critical steps are required for performing successful NSE experiments and collecting high-quality data. A key step in ensuring the effective use of neutron beam time during an NSE experiment is to characterize the liposomal suspensions with lab-based methods prior to the NSE experiment. For exmaple, the size distribution (or diffusion constant) of extruded liposomes can be determined by dynamic light scattering (DLS), readily available in individual labs or in shared facilities[84]. Cryo-electron microscopy is another charcaterization method recently validated on liposomal samples, where high-resolution microscopy images on cryomicrotomed sections of liposomal suspension can be effectively used to examine liposomal unilamellarity[65], domain formation[85,86], or the incorporation of additives such as nanoparticles[76] and proteins[87]. Alternatively, small-angle x-ray scattering (SAXS) can be used to characterize the membrane structure[88], assess liposomal multilamellarity[65], or evaluate the effects of additives on membrane structural properties[89]. Besides these lab-based techniques, it is highly advisable that NSE measurements on liposomal samples are paired with structural studies using small-angle neutron scattering (SANS)[54,90]. SANS is an excellent complement to NSE, not only for acquiring structural membrane information but also for examining the intensity of the neutron scattering signal from the sample, confirming the contrast scheme, and making an informed choice about the Q-range over which the NSE measurements should be performed. Therefore, it is recommended that NSE users request SANS beamtime when applying for NSE experiments.

However, NSE suffers from sample limitations in studies of biological membranes. One of the major limiting factors of such experiments is the standard amount of sample required for NSE measurements (~4 mL) and the high sample concentrations amounting to ~200 mg of membrane material (lipids and proteins) to obtain high quality data. In many cases, the production of such amounts of biological material is not feasible or is cost prohibitive. In such scenarios, it is possible to reduce the concentration to 20–25 mg/mL, but this would require at least a 4-fold increase in the acquisition time in order to obtain comparable statistics to samples with 50 mg/mL concentrations. These stringent requirements on sample volume and concentration could be alleviated with the next generation of NSE spectrometers on higher-flux neutron sources, such as the second target station at Oak Ridge National Lab and the European Spallation Source. Another critical limitation in performing NSE experiments on lipid membranes requiring selective deuteration schemes is the lack of commercial availabilty of some deuterated variants of lipid molecules or their exorbitant prices, if available. In some cases, these limitations can be circumvented by requesting the synthesis of deuterated lipids (or cholesterol, proteins) through user deuteration facilities, such as the bio-deuteration lab at Oak Ridge National Lab, the national deuteration facility at ANSTO, or the deuteration facility at the ISIS Neutron and Muon Source. Access to these facilities and their synthesis capabilities is available through submitted user proposals which are peer-reviewed based on the scientific merit of the proposed material synthesis and its intended use in isotope-sensitive studies.

Despite these limitations, the application of NSE spectroscopy in studies of membrane mechanics has led to the determination of the bending rigidity moduli of membranes with various degrees

of complexity, from single-component lipid membranes[35,38] to multicomponent biomimetic membranes[41,66,91], all of which have advanced our understanding of the dynamic nature of lipid membranes. For instance, NSE bending rigidity measurements of lipid membranes with different molecular units, e.g., lipids of different acyl chain lengths and chain saturation[38,72,92], have provided essential information about the role of molecular chemistry in membrane mechanics. When paired with structural information, such as membrane thickness or molecular packing[93], these measurements start to provide new perspectives on the dependence between membrane structure and dynamics and how they influence membrane function. The mesoscopic scales of NSE uniquely position it for such fundamental investigations of structure-property relations, most relevant on the length scale of molecular assemblies. This topic was recently explored in two NSE studies on cholesterol-rich lipid membranes[36] and in binary lipid membranes with hydrophobic mismatch between the two lipid components[39]. Both studies found strong evidence that membrane mechanics scale with the area per lipid, corroborating the conclusions from a recent all-atom MD simulations by Doktorova et al.[82]. These findings emphasize the self-assembled nature of lipid membranes and provide a unifying picture of molecular packing as a key parameter in defining membrane dynamical and functional properties.

Other applications of NSE involve studies of the mechanical response of membranes to small additives, including biological molecules such as cholesterol[36,37], trehalose[92], and melittin[73,94], or inorganic additives such as nanoparticles for drug delivery applications[76]. NSE has also been used to understand how membrane mechanics respond to changes in their environment, including temperature[92], pH[74], and the presence of crowding macromolecules[95]. Such studies are contributing to a better understanding of the factors that influence the softening or stiffening of lipid membranes, under biological conditions related to health and disease, and in controlled settings for therapeutic applications. Notably, NSE measurements have also been used to probe the effect of antimicrobial peptides on membrane dynamics[73,94]. Further examples of NSE applications on biomembranes include studies of the dynamics of flattened membrane structures, called thylakoids, which house the photosynthetic machinery in cyanobacterial cells[96,97].

One can also utilize selective lipid deuteration in NSE studies to investigate the dynamics of specific membrane features that are relevant to biological function. For example, Nickels et al. used selective lipid deuteration in domain-forming lipid membranes to generate lateral contrast within the membrane, as previously illustrated by Heberle et al.[28]. This deuteration scheme enabled independent measurements of the bending rigidity of the lipid domains and the host lipid matrix[41] (see **Figure 2B**). The findings confirmed that the two membrane compartments have distinct bending rigidity moduli, which could be a driving mechanism for domain formation in cellular membranes. In a more recent study, Rickeard et al. used cyclodextrin exchange between protiated and deuterated liposomes to obtain asymmetric liposomes with isotopically labeled leaflets[40] (**Figure 2C**). Their end liposomes had a protiated leaflet and a deuterated leaflet that is contrast matched to the buffer, enabling studies of individual leaflet dynamics and providing a first direct experimental account of the effect of asymmetry and leaflet coupling on membrane bending fluctuations.

Selective membrane deuteration has also been used in NSE studies of membrane thickness fluctuations, a long predicted dynamic mode in lipid membranes[98] that was only recently observed with the advent of NSE spectroscopy[35,99]. These measurements utilize tail-deuterated membranes to amplify the signal from the membrane headgroup regions and resolve the thickness fluctuation signal. This type of NSE experiments is relatively recent, but it has been effectively used to understand the interdependence of membrane elastic and viscous properties[38], to explore the scaling of bending rigidity and viscosity with molecular packing in mixed lipid membranes[39], and to probe the local effects of cholesterol on membrane viscosity[36]. Another area of biological significance in which this dynamic mode could have far-reaching implications is mesoscopic membrane-protein interactions. It is known that the function of membrane proteins is tightly linked to hydrophobic matching between the protein and the host membrane. Thus, variations in membrane thickness, due to thickness fluctuations, could act as a regulatory mechanism for the function of membrane proteins. NSE is extremely well suited for such studies as it can directly probe the effects of protein binding and insertion on membrane thickness fluctuations. Recent NSE measurements from our group (unpublished) suggest that transmembrane protein insertion could significantly suppress membrane thickness fluctuations and could present a potential mechanism for regulating signaling events. This is a pressing, yet underdeveloped, area of research where NSE can have significant impact in understanding the dynamic responses of membranes to protein binding and insertion on the length and time scales of key biological functions imparted by the interactions of proteins with cell membranes.

In summary, NSE has evolved over the last few years as a powerful tool for interrogating membrane dynamics over spatial and temporal scales of vital biological functions. The technique is rapidly gaining widespread interest and its potential in answering key questions in membrane function is becoming well recognized. The contrast variation capabilities within NSE have positioned it as a unique approach to measure mesoscopic membrane properties that would otherwise be challenging to obtain. Another significant advantage of NSE over traditional spectroscopy methods in studies of membrane dynamics is its overlap with the length and time scales accessible with MD simulations, allowing for synergistic experimental/computation studies to gain a molecular level understanding of the different molecular components making up membranes. Despite its promise, there are still some limitations in the use of NSE in biological membrane studies, including the requirement for large sample volumes, the difficulty in selective deuteration in biological systems, and the relatively low neutron flux on NSE spectrometers, which results in longer measurement times and limited beamtime availability. However, these shortcomings could be overcome in the near future with constant developments in neutron sources and instrumentation along with advances in deuteration facilities.

ACKNOWLEDGMENTS:

R. Ashkar thanks M. Nagao, L.-R. Stingaciu, and P. Zolnierczuk for many useful discussions and for their frequent assistance with NSE experiments on their respective beamlines. The authors acknowledge the use of neutron spin echo spectrometers at NIST and ORNL. The NSE spectrometer at NIST is supported by the Center for High Resolution Neutron Scattering, a partnership between the National Institute of Standards and Technology and the National Science Foundation under agreement no. DMR-1508249. The NSE spectrometer at ORNL's

Spallation Neutron Source is supported by the Scientific User Facilities Division, Office of Basic Energy Sciences, US Department of Energy. Oak Ridge National Laboratory is managed by UT-Battelle, LLC under US DOE Contract No. DE-AC05-00OR22725.

DISCLOSURES:

The authors declare no conflicts of interest and have nothing to disclose.

REFERENCES:

1. Singer, S. J., Nicolson, G. L. The fluid mosaic model of the structure of cell membranes. *Science*. **175** (4023), 720–731 (1972).
2. Andersen, O. S., Koeppe, R. E. Bilayer thickness and membrane protein function: an energetic perspective. *Annual Review of Biophysics and Biomolecular Structure*. **36** 107–130 (2007).
3. Lundbæk, J. A., Collingwood, S. A., Ingólfsson, H. I., Kapoor, R., Andersen, O. S. Lipid bilayer regulation of membrane protein function: gramicidin channels as molecular force probes. *Journal of The Royal Society Interface*. **7** (44), 373–395 (2010).
4. Bradley, R. P., Radhakrishnan, R. Curvature–undulation coupling as a basis for curvature sensing and generation in bilayer membranes. *Proceedings of the National Academy of Sciences of the United States of America*. **113** (35), E5117–E5124 (2016).
5. Perozo, E., Cortes, D. M., Sompornpisut, P., Kloda, A., Martinac, B. Open channel structure of MscL and the gating mechanism of mechanosensitive channels. *Nature*. **418** (6901), 942–948 (2002).
6. Jensen, M. Ø., Mouritsen, O. G. Lipids do influence protein function—the hydrophobic matching hypothesis revisited. *Biochimica et Biophysica Acta (BBA) - Biomembranes*. **1666** (1–2), 205–226 (2004).
7. Rajendran, L., Simons, K. Lipid rafts and membrane dynamics. *Journal of Cell Science*. **118** (6), 1099–1102 (2005).
8. Katchalsky, A., Spangler, R. Dynamics of membrane processes. *Quarterly Reviews of Biophysics*. **1** (2), 127–175 (1968).
9. Rheinstädter, M. C. Collective molecular dynamics in proteins and membranes (Review). *Biointerphases*. **3** (2), FB83–FB90 (2008).
10. Fujiwara, T., Ritchie, K., Murakoshi, H., Jacobson, K., Kusumi, A. Phospholipids undergo hop diffusion in compartmentalized cell membrane. *The Journal of Cell Biology*. **157** (6), 1071–1082 (2002).
11. Hac, A. E., Seeger, H. M., Fidorra, M., Heimburg, T. Diffusion in two-component lipid membranes--a fluorescence correlation spectroscopy and monte carlo simulation study. *Biophysical Journal*. **88** (1), 317–333 (2005).
12. Heinrich, M., Tian, A., Esposito, C., Baumgart, T. Dynamic sorting of lipids and proteins in membrane tubes with a moving phase boundary. *Proceedings of the National Academy of Sciences of the United States of America*. **107** (16), 7208–7213 (2010).
13. Hormel, T. T., Kurihara, S. Q., Brennan, M. K., Wozniak, M. C., Parthasarathy, R. Measuring lipid membrane viscosity using rotational and translational probe diffusion. *Physical Review Letters*. **112** (18), 188101 (2014).

14. Dimova, R. Recent developments in the field of bending rigidity measurements on membranes. *Advances in Colloid and Interface Science*. **208**, 225–234 (2014).
15. Bassereau, P., Sorre, B., Lévy, A. Bending lipid membranes: Experiments after W. Helfrich's model. *Advances in Colloid and Interface Science*. **208**, 47–57 (2014).
16. Monzel, C., Sengupta, K. Measuring shape fluctuations in biological membranes. *Journal of Physics D: Applied Physics*. **49** (24), 243002 (2016).
17. Deserno, M. Mesoscopic membrane physics: concepts, simulations, and selected applications. *Macromolecular Rapid Communications*. **30** (9–10), 752–771 (2009).
18. Reynwar, B. J. et al. Aggregation and vesiculation of membrane proteins by curvature-mediated interactions. *Nature*. **447** (7143), 461–464 (2007).
19. Haswell, E. S., Phillips, R., Rees, D. C. Mechanosensitive channels: what can they do and how do they do it? *Structure*. **19** (10), 1356–1369 (2011).
20. Phillips, R., Ursell, T., Wiggins, P., Sens, P. Emerging roles for lipids in shaping membrane-protein function. *Nature*. **459** (7245), 379–385 (2009).
21. Dill, K. A., Chan, H. S. From Levinthal to pathways to funnels. *Nature Structural Biology*. **4** (1), 10–19 (1997).
22. Henzler-Wildman, K., Kern, D. Dynamic personalities of proteins. *Nature*. **450** (7172), 964–972 (2007).
23. Grimaldo, M., Roosen-Runge, F., Zhang, F., Schreiber, F., Seydel, T. Dynamics of proteins in solution. *Quarterly Reviews of Biophysics*. **52**, e7 (2019).
24. Lyman, E., Hsieh, C.-L., Eggeling, C. From dynamics to membrane organization: experimental breakthroughs occasion a “modeling manifesto”. *Biophysical Journal*. **115** (4), 595–604 (2018).
25. Arriaga, L. R. et al. Dissipative curvature fluctuations in bilayer vesicles: Coexistence of pure-bending and hybrid curvature-compression modes. *The European Physical Journal. E, Soft Matter*. **31** (1), 105–113 (2010).
26. Honerkamp-Smith, A. R., Veatch, S. L., Keller, S. L. An introduction to critical points for biophysicists; observations of compositional heterogeneity in lipid membranes. *Biochimica et Biophysica Acta (BBA) - Biomembranes*. **1788** (1), 53–63 (2009).
27. Veatch, S. L., Keller, S. L. Organization in lipid membranes containing cholesterol. *Physical Review Letters*. **89** (26), 268101 (2002).
28. Heberle, F. A. et al. Bilayer thickness mismatch controls domain size in model membranes. *Journal of the American Chemical Society*. **135** (18), 6853–6859 (2013).
29. Nickels, J. D. et al. The in vivo structure of biological membranes and evidence for lipid domains. *PLOS Biology*. **15** (5), e2002214 (2017).
30. Simons, K., Ikonen, E. Functional rafts in cell membranes. *Nature*. **387** (6633), 569–572 (1997).
31. van Meer, G., Voelker, D. R., Feigenson, G. W. Membrane lipids: where they are and how they behave. *Nature Reviews. Molecular Cell Biology*. **9** (2), 112–124 (2008).
32. Liu, S.-L. et al. Orthogonal lipid sensors identify transbilayer asymmetry of plasma membrane cholesterol. *Nature Chemical Biology*. **13**, 268 (2016).
33. Rothman, J., Lenard, J. Membrane asymmetry. *Science*. **195** (4280), 743–753 (1977).
34. Ashkar, R. et al. Neutron scattering in the biological sciences: progress and prospects. *Acta Crystallographica Section D*. **74** (12), 1129–1168 (2018).

35. Woodka, A. C., Butler, P. D., Porcar, L., Farago, B., Nagao, M. Lipid bilayers and membrane dynamics: insight into thickness fluctuations. *Physical Review Letters*. **109** (5), 058102 (2012).
36. Chakraborty, S. et al. How cholesterol stiffens unsaturated lipid membranes. *Proceedings of the National Academy of Sciences of the United States of America*. **117** (36), 21896–21905 (2020).
37. Arriaga, L. R. et al. Stiffening effect of cholesterol on disordered lipid phases: a combined neutron spin echo + dynamic light scattering analysis of the bending elasticity of large unilamellar vesicles. *Biophysical Journal*. **96** (9), 3629–3637 (2009).
38. Nagao, M., Kelley, E. G., Ashkar, R., Bradbury, R., Butler, P. D. Probing elastic and viscous properties of phospholipid bilayers using neutron spin echo spectroscopy. *The Journal of Physical Chemistry Letters*. **8** (19), 4679–4684 (2017).
39. Kelley, E. G., Butler, P. D., Ashkar, R., Bradbury, R., Nagao, M. Scaling relationships for the elastic moduli and viscosity of mixed lipid membranes. *Proceedings of the National Academy of Sciences of the United States of America*. **117** (38), 23365–23373 (2020).
40. Rickeard, B. W. et al. Transverse lipid organization dictates bending fluctuations in model plasma membranes. *Nanoscale*. **12** (3), 1438–1447 (2020).
41. Nickels, J. D. et al. Mechanical properties of nanoscopic lipid domains. *Journal of the American Chemical Society*. **137** (50), 15772–15780 (2015).
42. Mezei, F. Neutron spin echo: A new concept in polarized thermal neutron techniques. *Zeitschrift für Physik A Hadrons and Nuclei*. **255** (2), 146–160 (1972).
43. Hayter, J. B., Penfold, J. Neutron spin-echo integral transform spectroscopy. *Zeitschrift für Physik B Condensed Matter*. **35** (2), 199–205 (1979).
44. Monkenbusch, M., Richter, D. in *Neutrons in Soft Matter*. Wiley. ch6 eds Imae, T., Kanaya, T., Furusaka, M., Torikai, N.) 147–182 (2011).
45. Pynn, R. in *Neutron Spin Echo*. Springer Berlin Heidelberg. (eds Mezei, F., Pappas, C., Gutberlet, T.) 159–177 (2003).
46. Holderer, O. et al. The JCNS neutron spin-echo spectrometer J-NSE at the FRM II. *Measurement Science and Technology*. **19** (3), 034022 (2008).
47. Schleger, P. et al. The long-wavelength neutron spin-echo spectrometer IN15 at the Institut Laue-Langevin. *Physica B: Condensed Matter*. **241–243**, 164–165 (1997).
48. Holderer, O., Zolnierczuk, P., Pasini, S., Stingaciu, L., Monkenbusch, M. A better view through new glasses: Developments at the Jülich neutron spin echo spectrometers. *Physica B: Condensed Matter*. **562**, 9–12 (2019).
49. Farago, B. et al. The IN15 upgrade. *Neutron News*. **26** (3), 15–17 (2015).
50. Ashkar, R. Selective dynamics in polymeric materials: Insights from quasi-elastic neutron scattering spectroscopy. *Journal of Applied Physics*. **127** (15), 151101 (2020).
51. Pasini, S., Holderer, O., Kozielewski, T., Richter, D., Monkenbusch, M. J-NSE-Phoenix, a neutron spin-echo spectrometer with optimized superconducting precession coils at the MLZ in Garching. *Review of Scientific Instruments*. **90** (4), 043107 (2019).
52. Svergun, D. I., Koch, M. H. J., Timmins, P. A., May, R. P. *Small Angle X-Ray and Neutron Scattering from Solutions of Biological Macromolecules*. Oxford University Press (2013).
53. Eicher, B. et al. Joint small-angle X-ray and neutron scattering data analysis of asymmetric lipid vesicles. *Journal of Applied Crystallography*. **50** (2), 419–429 (2017).

54. Heberle, F. A. et al. Model-based approaches for the determination of lipid bilayer structure from small-angle neutron and X-ray scattering data. *European Biophysics Journal*. **41** (10), 875–890 (2012).
55. Jaksch, S., Koutsioubas, A., Mattauch, S., Holderer, O., Frielinghaus, H. Long-range excitations in phospholipid membranes. *Chemistry and Physics of Lipids*. **225**, 104788 (2019).
56. Jaksch, S. et al. Influence of ibuprofen on phospholipid membranes. *Physical Review E*. **91** (2), 022716 (2015).
57. Armstrong, C. L. et al. Effect of cholesterol on the lateral nanoscale dynamics of fluid membranes. *European Biophysics Journal*. **41** (10), 901–913 (2012).
58. Rheinstädter, M. C., Häußler, W., Salditt, T. Dispersion relation of lipid membrane shape fluctuations by neutron spin-echo spectrometry. *Physical Review Letters*. **97** (4), 048103 (2006).
59. Armstrong, C. L., Häußler, W., Seydel, T., Katsaras, J., Rheinstädter, M. C. Nanosecond lipid dynamics in membranes containing cholesterol. *Soft Matter*. **10** (15), 2600–2611 (2014).
60. Nickels, J. D. et al. Lipid rafts: buffers of cell membrane physical properties. *The Journal of Physical Chemistry B*. **123** (9), 2050–2056 (2019).
61. Michonova-Alexova, E. I., Sugár, I. P. Component and state separation in DMPC/DSPC lipid bilayers: a Monte Carlo simulation study. *Biophysical Journal*. **83** (4), 1820–1833 (2002).
62. Sugár, I. P., Thompson, T. E., Biltonen, R. L. Monte Carlo simulation of two-component bilayers: DMPC/DSPC mixtures. *Biophysical Journal*. **76** (4), 2099–2110 (1999).
63. Mabrey, S., Sturtevant, J. M. Investigation of phase transitions of lipids and lipid mixtures by sensitivity differential scanning calorimetry. *Proceedings of the National Academy of Sciences*. **73** (11), 3862–3866 (1976).
64. *Neutron activation and scattering calculator*, <https://www.ncnr.nist.gov/resources/activation/>.
65. Scott, H. L. et al. On the mechanism of bilayer separation by extrusion, or why your LUVs are not really unilamellar. *Biophysical Journal*. **117** (8), 1381–1386 (2019).
66. Ashkar, R. et al. Tuning membrane thickness fluctuations in model lipid bilayers. *Biophysical Journal*. **109** (1), 106–112 (2015).
67. Carrillo, J.-M. Y., Katsaras, J., Sumpter, B. G., Ashkar, R. A computational approach for modeling neutron scattering data from lipid bilayers. *Journal of Chemical Theory and Computation*. **13** (2), 916–925 (2017).
68. Azuah, R. T. et al. DAVE: a comprehensive software suite for the reduction, visualization, and analysis of low energy neutron spectroscopic data. *Journal of Research of the National Institute of Standards and Technology*. **114** (6), 341–358 (2009).
69. Van Hove, L. Correlations in space and time and born approximation scattering in systems of interacting particles. *Physical Review*. **95** (1), 249–262 (1954).
70. Zilman, A. G., Granek, R. Undulations and dynamic structure factor of membranes. *Physical Review Letters*. **77** (23), 4788–4791 (1996).
71. Kelley, E. G., Butler, P. D., Nagao, M. Collective dynamics in model biological membranes measured by neutron spin echo spectroscopy, Walter de Gruyter, Inc. 131–176 (2019).
72. Zheng, Y., Michihiro, N., Dobrin, P. B. Bending elasticity of saturated and monounsaturated phospholipid membranes studied by the neutron spin echo technique.

Journal of Physics: Condensed Matter. **21** (15), 155104 (2009).
73. Sharma, V. K.,Qian, S. Effect of an antimicrobial peptide on lateral segregation of lipids: a structure and dynamics study by neutron scattering. *Langmuir*. **35** (11), 4152–4160 (2019).
74. Boggara, M. B., Faraone, A., Krishnamoorti, R. Effect of pH and Ibuprofen on the Phospholipid Bilayer Bending Modulus. *The Journal of Physical Chemistry B*. **114** (24), 8061–8066 (2010).
75. Lee, J.-H. et al. Thermal fluctuation and elasticity of lipid vesicles interacting with pore-forming peptides. *Physical Review Letters*. **105** (3), 038101 (2010).
76. Chakraborty, S., Abbasi, A., Bothun, G. D., Nagao, M., Kitchens, C. L. Phospholipid bilayer softening due to hydrophobic gold nanoparticle inclusions. *Langmuir*. **34** (44), 13416–13425 (2018).
77. Hoffmann, I. et al. Softening of phospholipid membranes by the adhesion of silica nanoparticles – as seen by neutron spin-echo (NSE). *Nanoscale*. **6** (12), 6945–6952 (2014).
78. Watson, M. C., Brown, Frank, L. H. Interpreting membrane scattering experiments at the mesoscale: the contribution of dissipation within the bilayer. *Biophysical Journal*. **98** (6), L9–L11 (2010).
79. Seifert, U., Langer, S. A. Viscous modes of fluid bilayer membranes. *Europhysics Letters (EPL)*. **23** (1), 71–76 (1993).
80. Bingham, R. J., Smye, S. W., Olmsted, P. D. Dynamics of an asymmetric bilayer lipid membrane in a viscous solvent. *EPL (Europhysics Letters)*. **111** (1), 18004 (2015).
81. Rawicz, W., Olbrich, K. C., McIntosh, T., Needham, D., Evans, E. Effect of chain length and unsaturation on elasticity of lipid bilayers. *Biophysical Journal*. **79** (1), 328–339 (2000).
82. Doktorova, M., LeVine, M. V., Khelashvili, G., Weinstein, H. A new computational method for membrane compressibility: bilayer mechanical thickness revisited. *Biophysical Journal*. **116** (3), 487–502 (2019).
83. Evans, E., Needham, D. Physical properties of surfactant bilayer membranes: thermal transitions, elasticity, rigidity, cohesion and colloidal interactions. *The Journal of Physical Chemistry*. **91** (16), 4219–4228 (1987).
84. Lesieur, S., Grabielle-Madelmont, C., Paternostre, M. T., Ollivon, M. Size analysis and stability study of lipid vesicles by high-performance gel exclusion chromatography, turbidity, and dynamic light scattering. *Analytical Biochemistry*. **192** (2), 334–343 (1991).
85. Heberle, F. A. et al. Direct label-free imaging of nanodomains in biomimetic and biological membranes by cryogenic electron microscopy. *Proceedings of the National Academy of Sciences of the United States of America*. **117** (33), 19943–19952 (2020).
86. Cornell, C. E., Mileant, A., Thakkar, N., Lee, K. K., Keller, S. L. Direct imaging of liquid domains in membranes by cryo-electron tomography. *Proceedings of the National Academy of Sciences of the United States of America*. **117** (33), 19713–19719 (2020).
87. Yao, X., Fan, X., Yan, N. Cryo-EM analysis of a membrane protein embedded in the liposome. *Proceedings of the National Academy of Sciences of the United States of America*. **117** (31), 18497–18503 (2020).
88. Kučerka, N., Nieh, M.-P., Katsaras, J. Fluid phase lipid areas and bilayer thicknesses of commonly used phosphatidylcholines as a function of temperature. *Biochimica et Biophysica Acta (BBA) - Biomembranes*. **1808** (11), 2761–2771 (2011).

89. Nielsen, J. E., Bjørnestad, V. A., Lund, R. Resolving the structural interactions between antimicrobial peptides and lipid membranes using small-angle scattering methods: the case of indolicidin. *Soft Matter*. **14** (43), 8750–8763 (2018).
90. Kučerka, N. et al. Lipid bilayer structure determined by the simultaneous analysis of neutron and X-ray scattering data. *Biophysical Journal*. **95** (5), 2356–2367 (2008).
91. Kelley, E. G., Butler, P. D., Nagao, M. Scaling of lipid membrane rigidity with domain area fraction. *Soft Matter*. **15** (13), 2762–2767 (2019).
92. Brüning, B.-A. et al. Bilayer undulation dynamics in unilamellar phospholipid vesicles: Effect of temperature, cholesterol and trehalose. *Biochimica et Biophysica Acta (BBA) - Biomembranes*. **1838** (10), 2412–2419 (2014).
93. Kučerka, N. et al. Areas of monounsaturated diacylphosphatidylcholines. *Biophysical Journal*. **97** (7), 1926–1932 (2009).
94. Sharma, V. K., Mamontov, E., Anunciado, D. B., O'Neill, H., Urban, V. S. Effect of antimicrobial peptide on the dynamics of phosphocholine membrane: role of cholesterol and physical state of bilayer. *Soft Matter*. **11** (34), 6755–6767 (2015).
95. Yu, J. et al. Structure and dynamics of lipid membranes interacting with antivirulence end-phosphorylated polyethylene glycol block copolymers. *Soft Matter*. **16** (4), 983–989 (2020).
96. Stingaciu, L.-R. et al. Revealing the dynamics of thylakoid membranes in living cyanobacterial cells. *Scientific Reports*. **6** (1), 19627 (2016).
97. Stingaciu, L.-R., O'Neill, H. M., Liberton, M., Pakrasi, H. B., Urban, V. S. Influence of chemically disrupted photosynthesis on cyanobacterial thylakoid dynamics in synechocystis sp. PCC 6803. *Scientific Reports*. **9** (1), 5711 (2019).
98. Miller, I. R. Energetics of fluctuation in lipid bilayer thickness. *Biophysical Journal*. **45** (3), 643–644 (1984).
99. Nagao, M. Observation of local thickness fluctuations in surfactant membranes using neutron spin echo. *Physical Review E*. **80** (3), 031606 (2009).

Figure 1

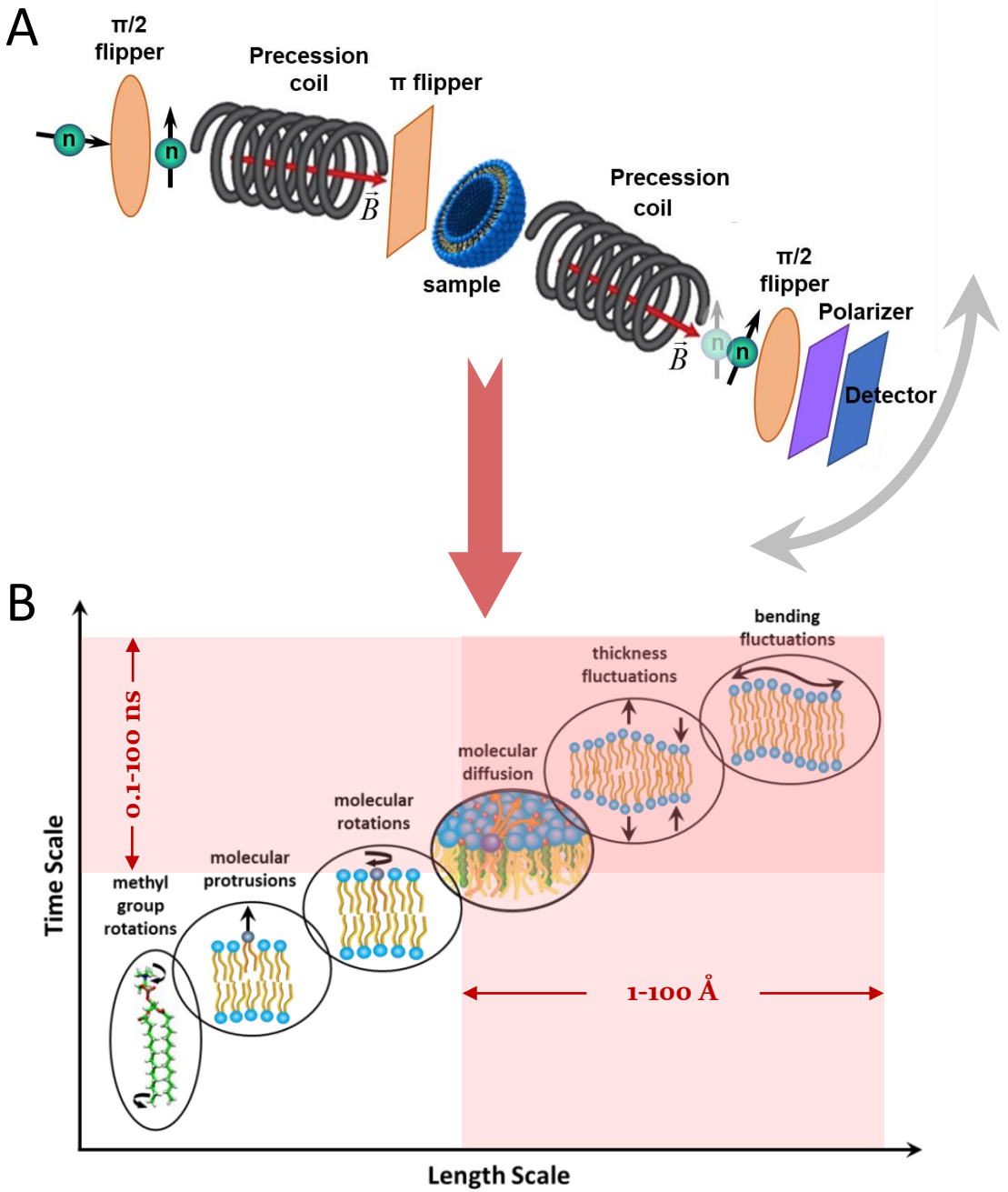

Figure 2

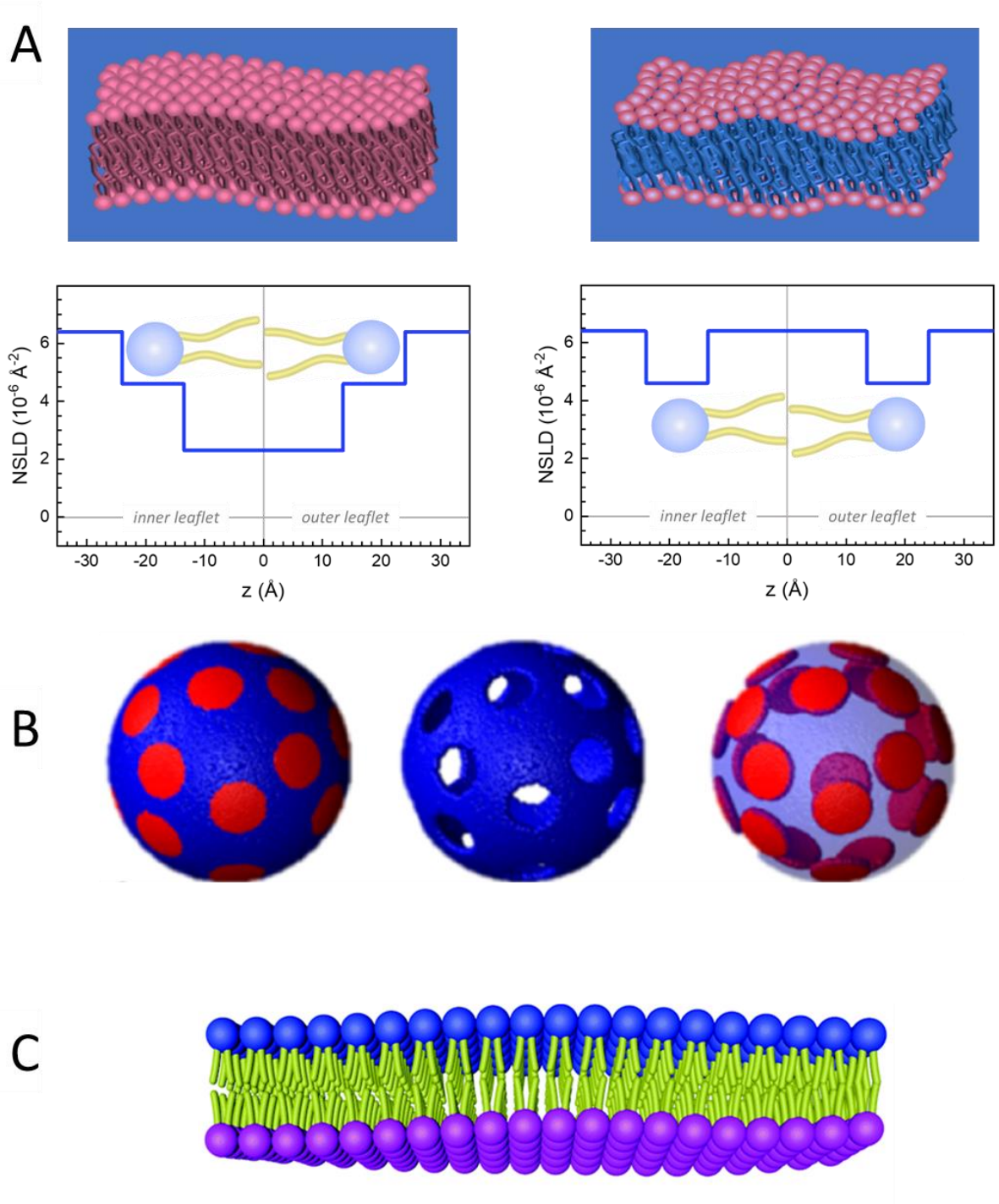

Figure 3

Click here to access/download;Figure;Figure3.pdf

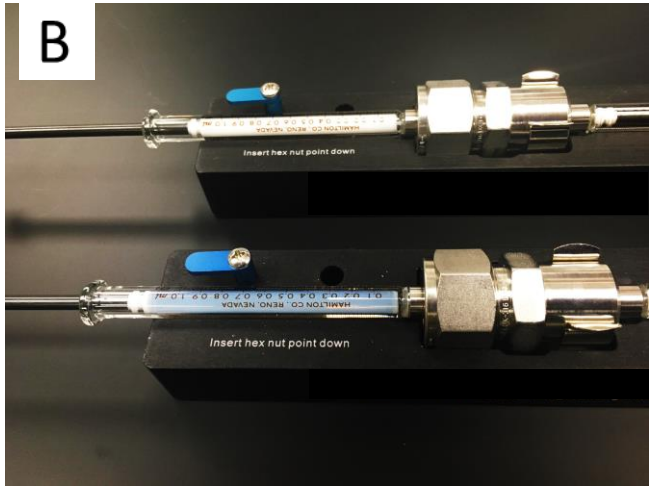

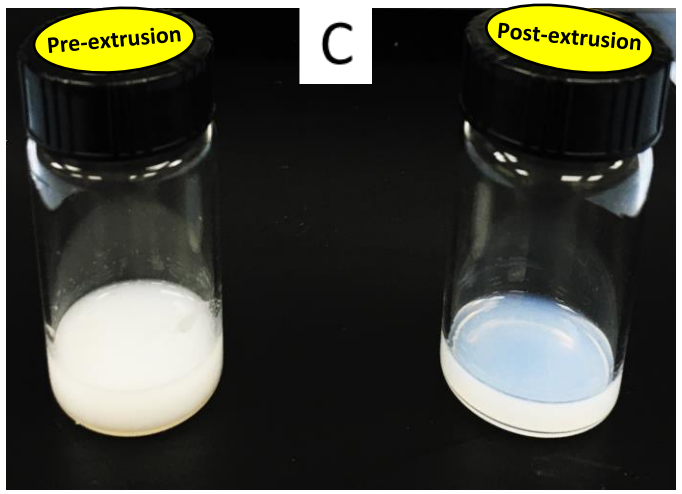

(A)

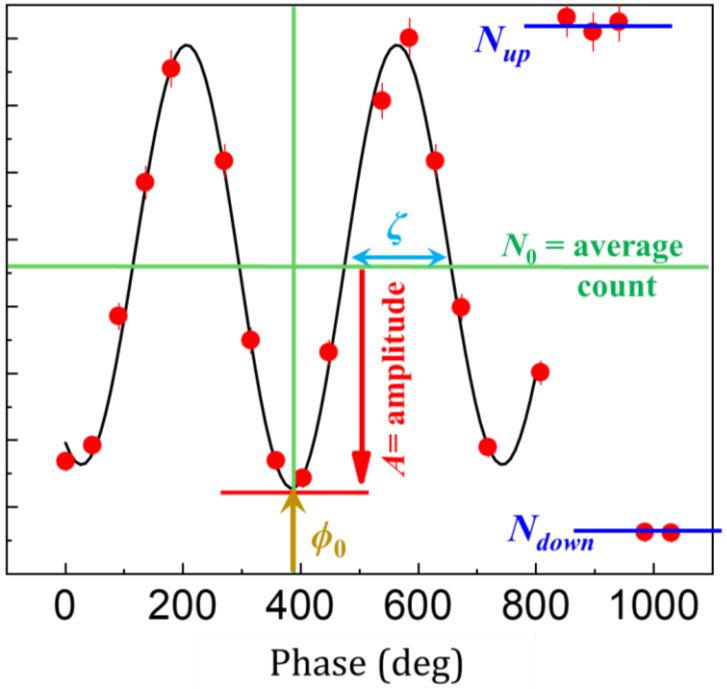

(B)

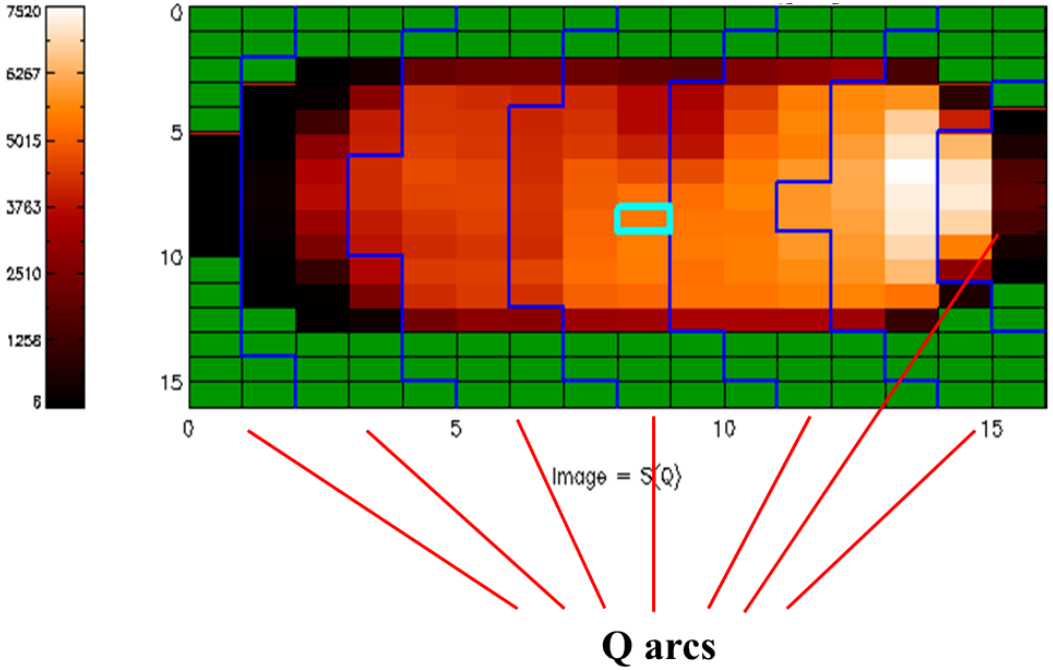

Figure 5

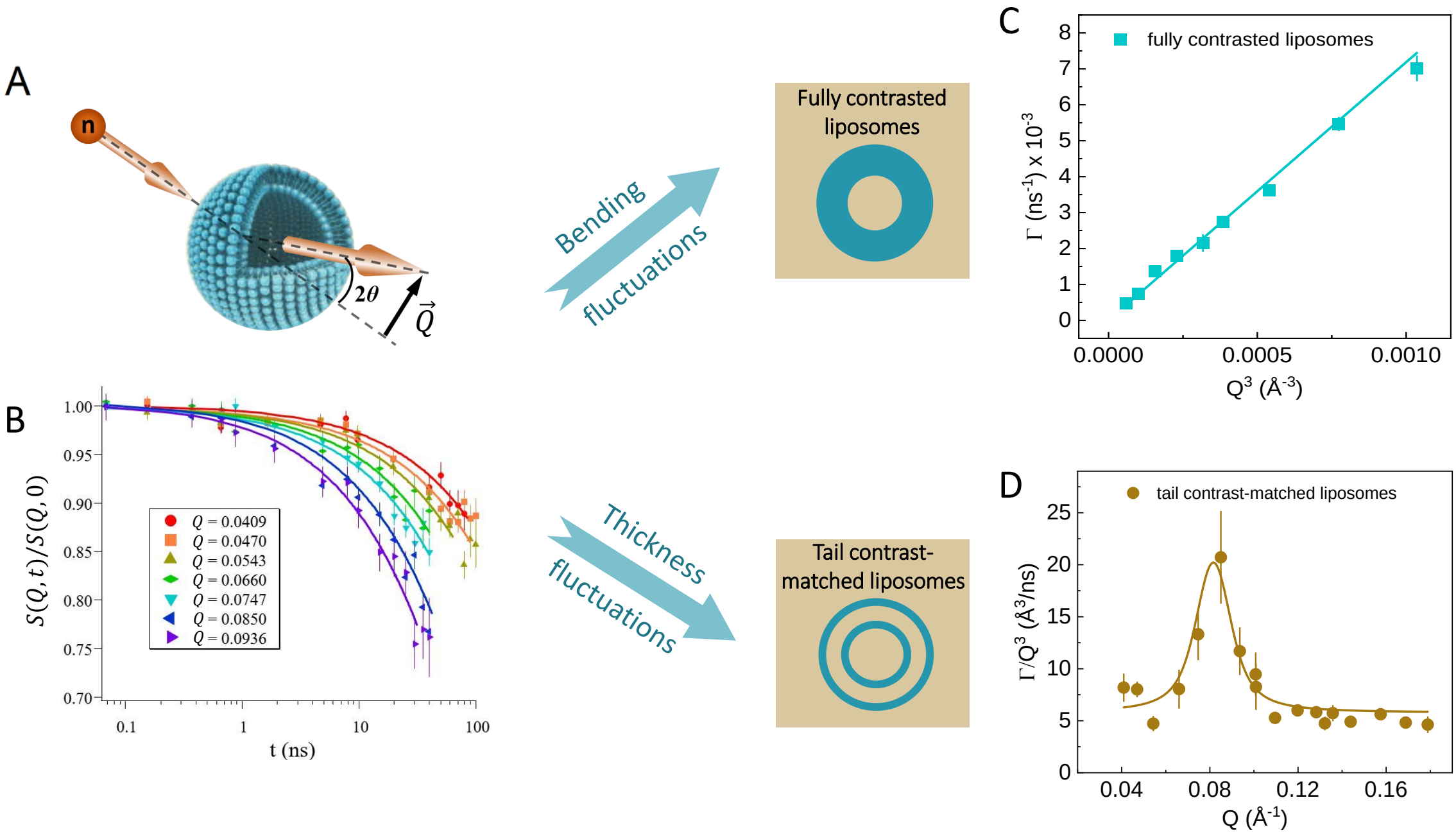

Table of Materials

Click here to access/download;Table of Materials;JoVE_Materials (5).xls

Name of Material/ Equipment	Company	Catalog Number
Chloroform (biotech grade)	Sigma Aldrich	496189
Circulating water bath	Julabo	SE-12
Deuterium Oxide	Cambridge Isotopes Laboratories	DLM-4
Digital Semi-Microbalance	Mettler Toledo	MS105
Ethanol (molecular biology grade)	Sigma Aldrich	E7023
Glass Pipets	VWR	36360-536
Glass Vials	Thermo Scientific	B7990-1
Lab grade freezer	Fisher Scientific	IU2886D
Lipids (protaited or perdeuterated)	Avanti Polar Lipids	varies by lipid
Millipore water purifier	Millipore Sigma	ZRQSVP3US
Mini Extruder Set	Avanti Polar Lipids	610020
Quick Connect Fittings	Grainger	2YDA1 and 2YDA7
Syringe Pump	SyringePump.com	New Era-1000
Ultrasonic bath	Fisher Scientific	CPX2800
Vacuum Oven	Thermo Scientific	3608
Vortex Mixer	Fisher Scientific	02-215-414

Comments/Description

Biotech. grade, ≥99.8%, contains 0.5-1.0% ethanol as stabilizer

Heating Circulator with smart pump, programmable temperature settings, and external sensor connection for measurement and control

Deuterated water; Heavy water (D_2O) (D, 99.9%)

Semi-micro balance with 120 g capacity, 0.01 mg readability, high resolution weighing cell, ergonomic doors, and pipette-check application

200 proof ethanol for molecular biology applications

Disposable Soda Lime glass Pasteur pipets

Borosilicate glass vials with PTFE/Silione septum caps

Ultra-low temprature freezer (-86 to -50 C) for long-term storage of lipids and proteins

Lipids can be purchased from Avanti in powder form or in a chloroform solution with the required amounts and deuteration schemes.

Direct-Q® 3 UV Water Purification System which deliver both pure and ultrapure water with a built-in UV lamp to reduce the levels of organic

Mini-extruder set includes mini-extruder, heating block, 2 GasTight Syringes, and 2 O-rings, Polycarbonate Membranes, and Filter Supports

Push-button tube fittings for QuickConnect water circulation applications, e.g. high temperature vesicle extrusion

Fully programmable syringe pump for infusion and withdrawal; programs up to 41 pumping phases with adjustable pumping rates, dispensed

Temperature controlled ultra sonic bath with programmable functionality for degassing and ultrasonic applications

0.7 cu ft vaccum oven with built-in-high-limit thermostat guards against overheating

Variable speed, analog control that allows low rpm start-up for gentle shaking or high-speed mixing for vigorous vortexing of samples

:s for biological applications

l volumes, and extrusion cycles

Editorial comments:

1. Please take this opportunity to thoroughly proofread the manuscript to ensure that there are no spelling or grammar issues.

We have proofread the paper and corrected spelling and grammar mistakes where observed.

2. Please provide an institutional email address for each author.

We have provided the email addresses of the two other authors.

3. Please revise the text to avoid the use of any personal pronouns (e.g., "we", "you", "our" etc.).

We have revised the text and restructured sentences initially written with personal pronouns.

4. JoVE cannot publish manuscripts containing commercial language. Please remove all commercial language from your manuscript and use generic terms instead. All commercial products should be sufficiently referenced in the Table of Materials: e.g., Whatman, Avanti mini extruder, Julabo, QuickConnect, etc. We must maintain our scientific integrity and prevent the subsequent video from becoming a commercial advertisement.

We apologize for this oversight. We have removed all mentions of commercial products and provided this information in the Table of Materials.

5. Please ensure that all text in the protocol section is written in the imperative tense as if telling someone how to do the technique (e.g., “Do this,” “Ensure that,” etc.). The actions should be described in the imperative tense in complete sentences wherever possible. Avoid usage of phrases such as “could be,” “should be,” and “would be” throughout the Protocol. Any text that cannot be written in the imperative tense may be added as a “Note.” However, notes should be concise and used sparingly. Please include all safety procedures and use of hoods, etc.

We have revised the protocol section and changed the sentence structures to address the requested changes.

6. Please note that your protocol will be used to generate the script for the video and must contain everything that you would like shown in the video. Please add more details to your protocol steps. Please ensure you answer the “how” question, i.e., how is the step performed? Alternatively, add references to published material specifying how to perform the protocol action. Please add more specific details (e.g., volume of samples/ buffers used, specification of the vials, numerical values for settings, etc.) to your protocol steps. There should be enough detail in each step to supplement the actions seen in the video so that viewers can easily replicate the protocol. Please move the discussion about the protocol to the Discussion.

We tried to provide additional details in the protocol. We hope that the additions will help clarify the protocol better and provide the necessary information for replication.

7. Line 186/248: Please use standard abbreviations when the unit is preceded by a numeral. Abbreviate liters to L to avoid confusion. Examples: 10 mL, 8 µL, 7 cm2

We have made the requested changes in the used units.

8. Please include a one-line space between each protocol step and highlight up to 3 pages of the Protocol (including headings and spacing) that identifies the essential steps of the protocol for the video, i.e., the steps that should be visualized to tell the most cohesive story of the Protocol. Remember that non-highlighted Protocol steps will remain in the manuscript, and therefore will still be available to the reader.

We have highlighted the parts of the manuscript that are essential for the video production.

9. Please remove the titles and Figure Legends from the embedded figures. Please include a Figure Legends section at the end of the Representative Results. The information provided in the Figure Legends after the Representative Results is sufficient.

We have provided higher-resolution versions of the figures and removed all figure legends from the figure file.

10. Please remove the embedded figure(s) from the manuscript. All figures should be uploaded separately to your Editorial Manager account. Each figure must be accompanied by a title and a description after the Representative Results of the manuscript text.

We have removed all figures from the manuscript and included the figure captions after the Representative Results section of the manuscript.

11. Please ensure that the references appear as the following: [Lastname, F.I., LastName, F.I., LastName, F.I. Article Title. Source. Volume (Issue), FirstPage – LastPage (YEAR).] For more than 6 authors, list only the first author then et al.

We have changed the reference style to adhere with JOVE's formating. To do this, we imported the JOVE Style into EndNote which automatically updated the citations to the required style.

12. Please obtain explicit copyright permission to reuse any figures from a previous publication. Explicit permission can be expressed in the form of a letter from the editor or a link to the editorial policy that allows re-prints. Please upload this information as a .doc or .docx file to your Editorial Manager account. The Figure must be cited appropriately in the Figure Legend, i.e. "This figure has been modified from [citation]."

We have obtained copyright permissions for adapted images shown in figures 2 and 4. We have deleted the reference in figure 5 as it shows generic data trends obtained with different deuteration schemes. However, since this figure now shows data that was unpublished before in this given format, we have included a statement acknowledging the use of the NIST NSE spectrometer for the collection of the data.

13. Figure 3: Please remove the commercial names from the figure and use generic names instead (e.g., SyringePump, Avanti polar lipids, Inc).

We have masked all commercial names in the figure and used generic descriptors in the figure caption.

14. Figure 4: Please define the units of Phase current within parenthesis in the X-axis.

We have revised this figure and changed the axis label to “Phase” expressed in degrees. We also included a clarification in the text (protocol 4.7) and in the figure caption.

15. Please provide a detailed list of chemicals, consumables and equipment used in the Table of Materials and sort them in alphabetical order.

We have updated the Table to Materials and included a complete list of chemicals, consumables, and equipment needed in the protocol.

Reviewers' comments:

Reviewer #1:
Manuscript Summary:

In their manuscript entitled "Neutron Spin Echo Spectroscopy: A Unique Probe for Lipid Membrane Dynamics and Membrane-Protein Interactions" the authors describe a protocol for running a Neutron Spin Echo measurement on liposomes of more or less homogeneous size. In their introduction they briefly talk about alternative techniques and introduce the technique of Spin Echo Spectroscopy in general. The discussion part summarizes the findings on the dynamics found in liposomes by previous studies.
The manuscript nicely describes the experimental requirements for a successful NSE-Experiment on liposomes. It also shows the potential of isotopic labelling. It falls short, when it comes to the aspect of the incorporation of proteins into the liposomes. And there is only one sentence on the effect of Membrane Proteins on the dynamics. Therefore, the title should be changed to " Neutron Spin Echo Spectroscopy: A Unique Probe for liposomal Lipid Membrane Dynamics"

We thank the Reviewer for his/her thorough review of the manuscript. The comments, suggestions, and recommendations s/he provided are very much appreciated and we believe that they have been tremendously helpful in improving the quality of the paper.

We also appreciate the Reviewer's comment about the title and the brief description of protein-membrane interactions. Given that the main focus of the paper is on membrane dynamics, we hoped to emphasize that NSE studies on membranes can also be used to understand the effect(s) of proteins incorporation on membrane dynamics. In such studies, and in the absence of membrane contrast matching, NSE primarily detects membrane dynamics (especially when measured with typical lipid:peptide ratios where peptides/proteins are the minority component). This area is currently underdeveloped, despite its strong biological relevance and its importance in membrane functions. Our intent is to illustrate in this paper that the same (or similar) NSE approaches as the ones applied on vesicular membranes can indeed be utilized in the studies of membrane dynamics in response to protein binding and insertion -- a topic of interest to a wider scientific community who would benefit from learning the potential of NSE in membrane-protein systems.

Major Concerns:

All Figures should be given in a vector graphic format or at least in a higher resolution as present in the manuscript.

We have uploaded higher resolution figures for the final publication. The figures that were embedded in the initial manuscript were meant to aid in the review process (being placed close to where they are referenced).

In the discussion or introduction one should also mention the technique of GINSES as found for example in the following publication:

Influence of ibuprofen on phospholipid membranes; Sebastian Jaksch, Frederik Lipfert, Alexandros Koutsioubas, Stefan Mattauch, Olaf Holderer, Oxana Ivanova, and Henrich Frielinghaus, PHYSICAL REVIEW E 91, 022716 (2015),

We thank the Reviewer for bringing this to our attention. While we explicitly state at the end of the introduction that this paper is focused on the dynamics of free-standing vesicular membranes, we can see the value of referring readers to other methods like GINSES for systems where supported membranes are required for measurements of in-plane dynamics. Therefore, we have added a couple of references on the GINSES approach including the paper recommended by the Reviewer.

On page 3 in line 111 one should also mention the J-NSE Phoenix instrument at the MLZ with an accessible Fourier-time of at least 350 ns, citing the following publication: J-NSE-Phoenix, a neutron spin-echo spectrometer with optimized superconducting precession coils at the MLZ in Garching; S. Pasini, O. Holderer, T. Kozielewski, D. Richter, and M. Monkenbusch, Rev. Sci. Instrum. 90, 043107 (2019); doi: 10.1063/1.5084303
Speaking with the instrument responsible, Olaf Holderer, even 420 ns are obtainable with a reasonable resolution signal of greater than 0.2=R.

The Reviewer makes an excellent point, and we apologize for this oversight. We agree that it is important to include the upgrades in the J-NSE spectrometer among recent advances in NSE instrumentation. We have added that to the discussion along with the corresponding reference.

Minor Concerns:

Page 3, line 134: "Note that the that the..." should read "Note that the..."

We have corrected this typo.

Page 7, line 230: The term "peristaltic" is not applicable here, it is a pure syringe pump. A peristaltic pump squeezes a tube on two points distant from each other and moves the liquid between the two squeezing points forward by rotating a wheel. The term "peristaltic" should be omitted from the whole manuscript.

The Reviewer makes a valid point. We can see the confusion that the use of this term could cause. Therefore, we have deleted all occurrences of the term “peristaltic” from the manuscript.

Page 8, line 268: "NOTE: After the extrusion cycles are complete. The lipid solution should end up in..." should read " NOTE: After the extrusion cycles are complete, the lipid solution should end up in..."

We corrected the sentence structure.

Page 10, line 315: " if your can prepare your sample in..." should read "if you can prepare your sample in..."

The typo has been corrected.

Page 10, line 337: the (1) should be replaced by (2), because equation 2 is the one which is referred to.

We changed the reference to the correct equation.

Page 11, line 352: The letters R (for Reference) and BKG for Background should be explained in the text below the equation.

The acronyms were introduced and defined in 4.4 and 4.6. However, to avoid any confusion we added a short statement clarifying what the acronyms are and referring the reader to the corresponding section.

Page 11, Figure caption of Figure 4: line 3: "echo signal to eq. (2)" should read "echo signal using eq. (1)"

We implemented the proposed correction.

Page 11, Figure caption of Figure 4: line 5: " ...due to poor echo signals over. The..." should read "...due to poor echo signals. The..."

The typo has been corrected.

Page 14, line 424: a "the" should be added in front of "mesoscopic"

Done.

Figure 2A: Font size should be at least doubled for better reading.

The figure was reproduced with bigger fonts and higher resolution.

Figure 3: The use of the term "peristaltic" should be omitted.

As requested by the Reviewer, all occurrences of the term “peristaltic” were removed from the manuscript.

Figure 4A: The unit for the phase current should be given (Ampere?)

We thank the reviewer for pointing this out. The label of the axes should be “Phase” not “Phase Current” and the values are expressed in degrees. It is common in NSE data representation to refer to the phase, rather than the phase current. Since the phase current is proportional to the precession angle of the neutron spin (which is the physically relevant quantity in NSE), the phase current can be expressed as an angle. We have added the necessary clarification in the text (protocol 4.7) and figure caption, and we modified the axes label accordingly.

Reviewer #2:

Manuscript Summary:

The manuscript describes a visual experiment demonstrating neutron spin echo (NSE) spectroscopy as a unique probe for lipid membrane dynamics. This demonstration is separated in two essential parts: The protocol for the lipid vesicle sample preparation and the protocol for conducting the NSE experiment and analyzing and interpreting the resulting data.

We thank the Reviewer for his/her careful reading of the manuscript and for providing constructive comments which helped improve the readability of the paper.

Recommendation:

The manuscript is timely, useful, well-structured, and well-written. I recommend to publish the suggested visualized experiment subsequent to considering the following points:

We appreciate that the Reviewer finds this paper timely and informative. We hope that it will facilitate the use of NSE by the wider scientific community to solve problems that are pertinent to the understanding of the rich dynamics in biomembranes and their role in membrane functions.

- The author list does not include a neutron spin-echo instrument scientist. Since the demonstration seems to require access to either the NIST or SNS spin-echo spectrometers, should one of these colleagues be involved?

With all due respect, we do not think that this is an appropriate request. While one can see where this comment is stemming from, we would like to point out to the Reviewer that this paper was written in response to an invitation to the corresponding author, who is an expert on NSE and its applications in biomembranes. Nevertheless, we have reached out to an NSE instrument scientist and invited him to be part of this paper, but he declined for personal reasons. This said, we do not believe that we need to explain the author list or justify why colleagues who were not part of this invitation are not co-authors on this paper.

- The membrane protein studies are mentioned only very briefly in the actual protocol (notably only in item 2.2.).

We appreciate this observation by the Reviewer. We note that the protein protocol is not elaborate because the primary focus of this paper is membrane dynamics. Given that different protein solutions could require different preparation methods, we believe that going into such detail could cause a diversion from the main theme of the paper. Our intent behind including the section on protein is to inform the wider scientific community of the great potential that NSE has in exploring the dynamic signatures of biomembranes in response to protein binding or insertion. This is a pressing, yet underdeveloped, area of research where NSE can have significant impact in understanding the dynamic responses of membranes on the length and time scales of key biological functions imparted by the interactions of proteins with cell membranes.

Minor points:

l.134: Typo extra 'that the': 'Note that the that the NSE signal ...'

The typo has been fixed.

l.339: The authors refer to figure 4A, not 3A.

We thank the Reviewer for pointing this out. The reference to the figure has been corrected.

l.347: The authors refer to figure 4

We apologize for the confusion in figure numbering. This was a result of a problem in the automatic updating of figure references in the Word template. The reference to the figure has been fixed.

l.359: The authors refer to figure 4B

Please see the response above.

l.573: Along with reference 22, the following additional reference may be cited: M.Grimaldo et al., Quart.Rev.Biophys.52, e7, 2019, https://dx.doi.org/10.1017/S0033583519000027 (containing also some details on NSE and complementary techniques).

We thank the reviewer for pointing us towards this reference. We found it quite informative and we believe that it could also be a valuable resource for readers interested in complementary NSE studies of protein dynamics. Therefore, we added this reference to the list of citations.

Reviewer #3:
Accept

AIP PUBLISHING LICENSE
TERMS AND CONDITIONS

Feb 08, 2021

This Agreement between Virginia Tech -- Rana Ashkar ("You") and AIP Publishing ("AIP Publishing") consists of your license details and the terms and conditions provided by AIP Publishing and Copyright Clearance Center.

License Number	5004531365732
License date	Feb 08, 2021
Licensed Content Publisher	AIP Publishing
Licensed Content Publication	Journal of Applied Physics
Licensed Content Title	Selective dynamics in polymeric materials: Insights from quasi-elastic neutron scattering spectroscopy
Licensed Content Author	Rana Ashkar
Licensed Content Date	Apr 21, 2020
Licensed Content Volume	127
Licensed Content Issue	15
Type of Use	Journal/Magazine
Requestor type	Author (original article)

Format	Electronic
Portion	Figure/Table
Number of figures/tables	1
Title of new article	Neutron Spin Echo Spectroscopy: A Unique Probe for Lipid Membrane Dynamics and Membrane-Protein Interactions
Lead author	Rana Ashkar
Title of targeted journal	Journal of Visualized Experiments
Publisher	MyJove Corp
Expected publication date	Mar 2021
Portions	Fig. 7
Requestor Location	Virginia Tech 850 W Campus Dr 309 Robeson Hall Blacksburg, VA 24061 United States Attn: Virginia Tech
Total	0.00 USD

Terms and Conditions

AIP Publishing -- Terms and Conditions: Permissions Uses

AIP Publishing hereby grants to you the non-exclusive right and license to use and/or distribute the Material according to the use specified in your order, on a one-time basis, for the specified term, with a maximum distribution equal to the number that you have ordered. Any links or other content accompanying the Material are not the subject of this license.

1. You agree to include the following copyright and permission notice with the reproduction of the Material:"Reprinted from [FULL CITATION], with the permission of AIP Publishing." For an article, the credit line and permission notice must be printed on the first page of the article or book chapter. For photographs, covers, or tables, the notice may appear with the Material, in a footnote, or in the reference list.
2. If you have licensed reuse of a figure, photograph, cover, or table, it is your responsibility to ensure that the material is original to AIP Publishing and does not contain the copyright of another entity, and that the copyright notice of the figure, photograph, cover, or table does not indicate that it was reprinted by AIP Publishing, with permission, from another source. Under no circumstances does AIP Publishing purport or intend to grant permission to reuse material to which it does not hold appropriate rights.
   You may not alter or modify the Material in any manner. You may translate the Material into another language only if you have licensed translation rights. You may not use the Material for promotional purposes.
3. The foregoing license shall not take effect unless and until AIP Publishing or its agent, Copyright Clearance Center, receives the Payment in accordance with Copyright Clearance Center Billing and Payment Terms and Conditions, which are incorporated herein by reference.
4. AIP Publishing or Copyright Clearance Center may, within two business days of granting this license, revoke the license for any reason whatsoever, with a full refund payable to you. Should you violate the terms of this license at any time, AIP Publishing, or Copyright Clearance Center may revoke the license with no refund to you. Notice of such revocation will be made using the contact information provided by you. Failure to receive such notice will not nullify the revocation.
5. AIP Publishing makes no representations or warranties with respect to the Material. You agree to indemnify and hold harmless AIP Publishing, and their officers, directors, employees or agents from and against any and all claims arising out of your use of the Material other than as specifically authorized herein.
6. The permission granted herein is personal to you and is not transferable or assignable without the prior written permission of AIP Publishing. This license may not be amended except in a writing signed by the party to be charged.
7. If purchase orders, acknowledgments or check endorsements are issued on any forms containing terms and conditions which are inconsistent with these provisions, such inconsistent terms and conditions shall be of no force and effect. This document, including the CCC Billing and Payment Terms and Conditions, shall be the entire agreement between the parties relating to the subject matter hereof.

This Agreement shall be governed by and construed in accordance with the laws of the State of New York. Both parties hereby submit to the jurisdiction of the courts of New York County for purposes of resolving any disputes that may arise hereunder.

V1.2

Questions? customercare@copyright.com or +1-855-239-3415 (toll free in the US) or +1-978-646-2777.

Mechanical Properties of Nanoscopic Lipid Domains

Author: Jonathan D. Nickels, Xiaolin Cheng, Barmak Mostofian, et al
Publication: Journal of the American Chemical Society
Publisher: American Chemical Society
Date: Dec 1, 2015

PERMISSION/LICENSE IS GRANTED FOR YOUR ORDER AT NO CHARGE

This type of permission/license, instead of the standard Terms & Conditions, is sent to you because no fee is being charged for your order. Please note the following:

- Permission is granted for your request in both print and electronic formats, and translations.
- If figures and/or tables were requested, they may be adapted or used in part.
- Please print this page for your records and send a copy of it to your publisher/graduate school.
- Appropriate credit for the requested material should be given as follows: "Reprinted (adapted) with permission from (COMPLETE REFERENCE CITATION). Copyright (YEAR) American Chemical Society." Insert appropriate information in place of the capitalized words.
- One-time permission is granted only for the use specified in your request. No additional uses are granted (such as derivative works or other editions). For any other uses, please submit a new request.

If credit is given to another source for the material you requested, permission must be obtained from that source.

BACK CLOSE WINDOW

Copyright Clearance Center Marketplace™

Order Confirmation

Thank you, your order has been placed. An email confirmation has been sent to you. Your order license details and printable licenses will be available within 24 hours. Please access Manage Account for final order details.

This is not an invoice. Please go to manage account to access your order history and invoices.

CUSTOMER INFORMATION

Payment by invoice: You can cancel your order until the invoice is generated by contacting customer service.

Billing Address

Prof Rana Ashkar
Virginia Tech
850 W Campus Dr
309 Robeson Hall
Blacksburg, VA 24061
United States

+1 (540) 231-5243
ashkar@vt.edu

Customer Location

Prof Rana Ashkar
Virginia Tech
850 W Campus Dr
309 Robeson Hall
Blacksburg, VA 24061
United States

PO Number (optional)

N/A

Payment options

Invoice

PENDING ORDER CONFIRMATION

Confirmation Number: Pending

Order Date: 08-Feb-2021

1. Nanoscale

0.00 USD

Order license ID	Pending	**Publisher**	RSC Pub
ISSN	2040-3372	**Portion**	Image/photo/illustration
Type of Use	Republish in a journal/magazine		

LICENSED CONTENT

Publication Title	Nanoscale	**Country**	United Kingdom of Great Britain and Northern Ireland
Author/Editor	National Center for Nanoscience and Technology., Royal Society of Chemistry (Great Britain)	**Rightsholder**	Royal Society of Chemistry
		Publication Type	e-Journal
Date	01/01/2009	**URL**	http://www.rsc.org/Publishing/Journals/NR/index.asp
Language	English		

REQUEST DETAILS

Portion Type	Image/photo/illustration	**Distribution**	United States and Canada
Number of images / photos / illustrations	1	**Translation**	Original language of publication
Format (select all that apply)	Electronic	**Copies for the disabled?**	No
Who will republish the content?	Publisher, not-for-profit	**Minor editing privileges?**	No
Duration of Use	Life of current edition	**Incidental promotional use?**	No
Lifetime Unit Quantity	Up to 499	**Currency**	USD
Rights Requested	Main product		

NEW WORK DETAILS

Title	Neutron Spin Echo Spectroscopy: A Unique Probe for Lipid Membrane Dynamics and Membrane-Protein Interactions	**Publisher imprint**	N/A
		Expected publication date	2021-03-10
		Expected size (number of pages)	10
Author	Rana Ashkar	**Standard identifier**	N/A
Publication	Journal of Visualized Experiments		
Publisher	MyJove Corp		

ADDITIONAL DETAILS

Order reference number	N/A	**The requesting person / organization to appear on the license**	Rana Ashkar/ Virginia Tech

REUSE CONTENT DETAILS

Title, description or numeric reference of the portion(s)	N/A	**Title of the article/chapter the portion is from**	N/A
Editor of portion(s)	N/A		
Volume of serial or monograph	N/A		

Page or page range of portion	N/A	**Author of portion(s)**	National Center for Nanoscience and Technology.; Royal Society of Chemistry (Great Britain)
		Issue, if republishing an article from a serial	N/A
		Publication date of portion	2009-01-01

Total Items: 1

Total Due: 0.00 USD

Accepted: All Publisher and CCC Terms and Conditions